Analytic Properties of the Free Energy: the Tricritical Ising Model

Alessandro Mossa

Mathematical Physics Sector

SISSA - International School for Advanced Studies

Supervisor
Prof. Giuseppe Mussardo

Thesis submitted for the degree of
Doctor Philosophiæ in Mathematical Physics

Academic Year 2003-04

A Sara Virginia che sa perché

Contents

List of Figures

List of Tables

Chapter 1

Introduction

More than fifty years ago, Yang and Lee [1, 2] showed the importance of understanding the analytic structure of the free energy in the theory of phase transitions. They proved that the thermodynamical equation of state is completely determined by the distribution of roots of the partition function (or, equivalently, singularities of the free energy). Their papers inspired several lines of further research. I just note that, as far as the Ising model is concerned, the task of unveiling the analytic properties of the free energy has been completed, very recently, by Fonseca and Zamolodchikov [3]. They were able to substantiate the identification of the Yang–Lee edge singularity with the spinoidal point, thus unifying the high- and low-temperature descriptions.

The main tool of Fonseca and Zamolodchikov's analysis is the truncated free-fermion space approach, that gives numerical access to the lowest energy levels of the Ising field theory defined on a cylinder. A similar analysis can, in principle, be performed to study the next-to-the-simplest unitary minimal model, namely the tricritical Ising model (in the following frequently referred to by the acronym TIM). Due to the universality principle, the insight gathered by working on this conformal field theory and its perturbations applies to all tricritical phenomena in dimension two chracterized by the same $\mathbb{Z}_2$ symmetry of the order parameter.

In practice, however, the extension of Fonseca–Zamolodchikov's method is far by trivial because the tricritical Ising model possesses four primary fields that are relevant in the renormalization group sense, instead of two like in the Ising case. On technical ground, moreover, there is no free-fermion space available, so that one is forced to truncate the conformal space, thus employing a less powerful approximation. Anyway, some at least qualitative picture can be outlined: this is the subject of my Ph.D. thesis.

The first chapter is structured as follows: the physics of tricritical points is introduced by means of a lattice (Sec. 1.1) and a field theoretical (Sec. 1.2) realizations of the TIM universality class. Then the example of the Ising field theory illustrates why it is interesting to introduce a complex magnetic field and what kind of results one can expect to obtain (Sec. 1.3). The last section is devoted to sketch the layout of the following chapters.

1.1 Ising and Blume–Emery–Griffiths models

The Ising model is defined as follows: arrange in some regular lattice N variables s_i called *spins* allowed to take values ± 1, then to any given configuration $\{s\} \equiv \{s_i, i = 1, \ldots, N\}$ associate an energy

$$E_{\{s\}} = -J \sum_{\langle i,j \rangle} s_i s_j - H \sum_{i=1}^{N} s_i \, . \tag{1.1}$$

The symbol $\langle i, j \rangle$ means that the first sum is performed over pairs of spins that are directly linked in the lattice (nearest neighbours). The sign of the coupling J determines whether neighbouring spins tend to be aligned in the same direction ($J > 0$, ferromagnetic Ising model) or in the opposite one ($J < 0$, antiferromagnetic case), while H represents an external magnetic field.

The partition function, from which one can extract all thermodynamic quantities, is defined by

$$Z_N(\beta, H) = \sum_{\{s\}} e^{-\beta E_{\{s\}}} \, , \tag{1.2}$$

where β is the inverse of the absolute temperature and the sum runs over all possible 2^N configurations. The free energy per site is defined according to

$$F(\beta, H) = -\frac{1}{\beta} \lim_{N \to \infty} \frac{1}{N} \ln Z_N(\beta, H) \, , \tag{1.3}$$

where the limit $N \to \infty$ is called thermodynamic limit.

An evident feature of the model with $H = 0$ is its $\mathbb{Z}_2$ symmetry related to spin reversal. If the lattice dimension is greater than 1, then this symmetry is spontaneously broken: when the inverse temperature is greater than the critical value β_c, the spontaneous magnetization per site

$$\mathcal{M} = - \left. \frac{\partial F}{\partial H} \right|_{H=0} \tag{1.4}$$

is different by zero, signaling that a consistent portion of the spins result aligned in the same direction. Another less evident symmetry is the Kramers–Wannier duality [4, 5], relating the high-temperature disordered phase with the low-temperature ordered one.

A great number of variations have been played over this simple theme. The one that more concerns this work is due to Blume, Emery and Griffiths [6] and consists in allowing the spins to take also the value 0 in addition to ± 1, while consistently enlarging the possibility of interaction:

$$
\begin{aligned}
E_{\{s\}} = -J \sum_{\langle i,j \rangle} s_i s_j - H \sum_{i=1}^{N} s_i + \Delta \sum_{i=1}^{N} s_i^2 + \\
- K \sum_{\langle i,j \rangle} s_i^2 s_j^2 - H_3 \sum_{\langle i,j \rangle} s_i s_j (s_i + s_j) \,.
\end{aligned}
\tag{1.5}
$$

The interpretation of the newly introduced couplings depends on the physical system one is thinking about: I will have in mind an annealed dilution of the ferromagnetic ($J > 0$) Ising model, that is an Ising model with non magnetic impurities (vacancies, corresponding to value 0 of the spin variable) in thermal equilibrium with the spin system. In such a context, Δ is a chemical potential enhancing (if $\Delta > 0$) or depressing (if $\Delta < 0$) the presence of vacancies, H_3 is a third-order magnetic field, and K is a biquadratic exchange interaction. This model, originally designed to describe a multicomponent fluid mixture, has also been applied to the study of metamagnets, and nowadays stands as the paradigmatic example of tricriticality. The special case $H_3 = K = 0$ deserves particular attention and a name on its own: it is the Blume–Capel model, independently introduced by Blume [7] and Capel [8] in 1966.

Also the Blume–Emery–Griffiths model shows a $\mathbb{Z}_2$ symmetry for $H = H_3 = 0$, but this symmetry can be broken discontinuously (first-order phase transition) if $\Delta > \Delta_t$. The point (β_t, Δ_t) lies at the junction of a line of first-order with a line of second-order phase transitions (see Fig. 1.1), hence enjoys the coexistence of three phases and is called tricritical. The global phase diagram in the five dimensional space of couplings is quite complicated [10], but it is useful to mention the result of the mean field approximation analysis of its $H_3 = K = 0$ subspace. I will just state the results more useful for my purpose; a detailed treatment of the Blume–Emery–Griffiths model, together with a rich bibliography and a review of early studies on tricriticality can be found in Ref. [9].

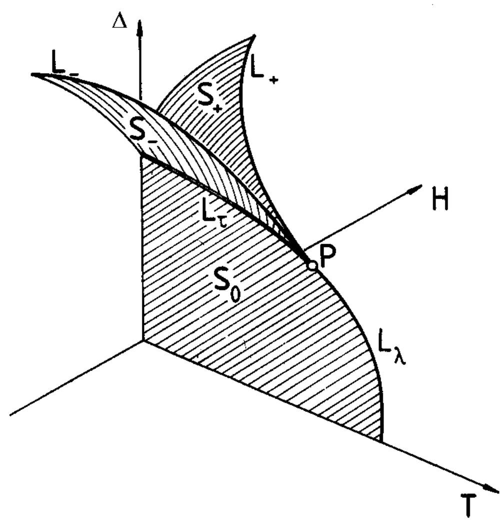

Figure 1.1: Qualitative phase diagram of the Blume–Capel model near the tricritical point P (from Ref. [9]): the lines L_+, L_-, L_λ are lines of critical points, while L_τ is a line of first-order phase transitions. On the surface S_0 we have coexistence of two ordered phases with opposite magnetization. The 'wing' S_+ (S_-) in the same way separates the phase with predominance of $s_i = 0$ from the phase with positive (negative) magnetization.

1.1.1 Mean field analysis of the Blume–Capel model

In the mean field approximation, a line of second order phase transitions (often called λ-line in literature) is given by

$$\begin{cases} \Delta_\lambda(\beta) = \dfrac{1}{\beta}\ln\left(2(\beta zJ-1)\right) \\ H_\lambda(\beta) = 0 \end{cases} \qquad 1 < \beta zJ < 3\,, \tag{1.6}$$

where z is the coordination number, that is the number of nearest neighbours each spin interacts with. At the tricritical point

$$\beta_t = \frac{3}{zJ} \qquad \Delta_t = \frac{2}{3}zJ\ln 2\,, \tag{1.7}$$

the λ-line meets two critical lines delimiting a pair of symmetrical coexistence surfaces (wings, see Fig. 1.1) identified by

$$\begin{cases} \Delta_\pm(\beta) = \dfrac{1}{2\beta}\ln\left(\dfrac{16}{4-\beta zJ}\right) \\ H_\pm(\beta) = \dfrac{1}{\beta}\ln\left(\dfrac{\beta zJ - 2 + \sqrt{\beta zJ(\beta zJ-3)}}{\sqrt{|(4-\beta zJ)|}}\right) \mp \dfrac{1}{\beta}\sqrt{\beta zJ(\beta zJ-3)} \end{cases}, \tag{1.8}$$

where $3 < \beta zJ < 4$. In the plane $H = 0$ the wings intersect in a line of first order phase transitions called τ-line which cannot be expressed in closed form.

If we now focus our attention on a small neighbourhood of the tricritical point, we can define the scaling fields

$$t = \frac{\beta_t}{\beta} - 1 \qquad \widetilde{\Delta} = \frac{1}{zJ}(\Delta - \Delta_t) + \nu t \qquad \widetilde{H} = \frac{H}{zJ}\,, \tag{1.9}$$

where we have introduced the constant $\nu = \frac{1}{2}(1 - \frac{4}{3}\ln 2) = 0.0379\ldots$. In the scaling limit $t \to 0$, Eq. (1.6) reads

$$\widetilde{\Delta}_\lambda(t) = -\frac{3}{8}t^2 + \mathcal{O}(t^3) \qquad \widetilde{H}_\lambda(t) = 0\,, \tag{1.10}$$

where $t > 0$ is understood, while Eq. (1.8) becomes

$$\widetilde{\Delta}_\pm(t) = \frac{3}{4}t^2 + \mathcal{O}(t^3) \qquad \widetilde{H}_\pm(t) = \pm\frac{6}{5}|t|^{5/2} + \mathcal{O}(t^3)\,, \tag{1.11}$$

and the τ-line is given by

$$\widetilde{\Delta}_\tau(t) = \frac{3}{32}t^2 + \mathcal{O}(t^3) \qquad \widetilde{H}_\tau(t) = 0\,. \tag{1.12}$$

Both Eq. (1.11) and Eq. (1.12) are valid for $t < 0$.

1.2 Landau–Ginzburg theory of tricriticality

The essential features of the theory of tricritical points can be qualitatively understood by considering a Landau–Ginzburg [11] formulation based on a scalar field $\Phi(x)$ (called order parameter in the theory of phase transitions). As to describe an ordinary critical point (like $(H = 0, \beta = \beta_c)$ in the Ising model) we need a quartic potential whose two degenerate vacua accounts for the two phases, so a tricritical point requires at least a sixth order potential which may display up to three minima:

$$\mathcal{A}_{LG} = \int d^D x \left[\frac{1}{2}(\partial_\mu \Phi)^2 + g_1 \Phi + g_2 \Phi^2 + g_3 \Phi^3 + g_4 \Phi^4 + \Phi^6 \right] . \qquad (1.13)$$

A term of order Φ^5 is absent because it can always be eliminated by a shift of the field $\Phi \to \Phi' + \Phi_0$, with a suitable choice of Φ_0.

If we set $g_1 = 0 = g_3$, thus considering only the $\mathbb{Z}_2$-symmetric subspace of couplings, we can easily realize that:

- if $g_2 > 0$ and $g_4 > 0$, then there is only one absolute minimum in $\Phi = 0$ (see Fig. 1.2(b));
- if $g_2 < 0$, then there are one relative maximum in $\Phi = 0$ and two absolute minima in $\Phi = \pm\sqrt{\frac{\sqrt{g_4^2 - 3g_2} - g_4}{3}}$ (see Fig. 1.2(c));
- if $g_4 < 0$, then there are three further possibilities:
  - if $g_2 > g_4^2/3$, then there is only one absolute minimum in $\Phi = 0$ (see Fig. 1.2(b));
  - if $g_4^2/4 < g_2 < g_4^2/3$, then there are one absolute minimum in $\Phi = 0$ and two relative minima in $\Phi = \pm\sqrt{\frac{\sqrt{g_4^2 - 3g_2} - g_4}{3}}$ (see Fig. 1.2(e));
  - if $0 < g_2 < g_4^2/4$, then there are one relative minimum in $\Phi = 0$ and two absolute minima in $\Phi = \pm\sqrt{\frac{\sqrt{g_4^2 - 3g_2} - g_4}{3}}$ (see Fig. 1.2(d)).

All the above informations are summarized in Fig. 1.2(a): the red line ($g_4 > 0$ while $g_2 = 0$) denotes second order phase transitions, characterized by the change of the potential from the shape of Fig. 1.2(b) to the one of Fig. 1.2(c), while the blue line ($g_4 < 0$ while $g_2 = g_4^2/4$) marks the first order phase transition, where the shape of the potential, in passing from Fig. 1.2(d) to Fig. 1.2(e), presents three degenerate minima (see Fig. 1.2(f)). The intersection $g_2 = 0 = g_4$ is a tricritical point. The analysis can be extended to the whole four dimensional space [12]: other critical submanifolds are found without spoiling the fact that the only tricritical point is defined by $g_1 = g_2 = g_3 = g_4 = 0$.

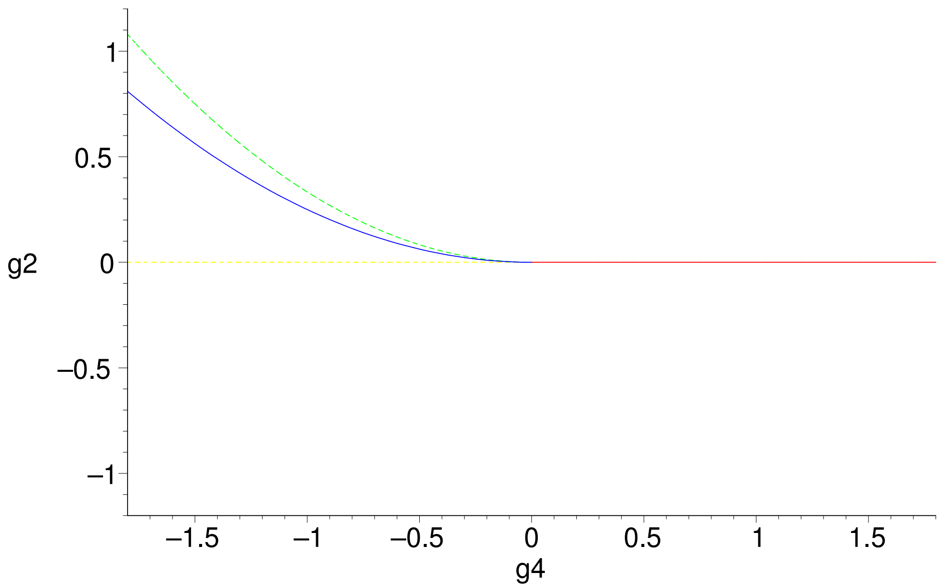

(a)

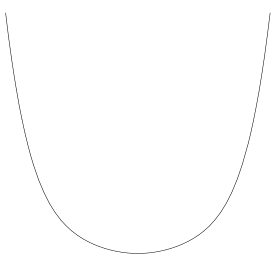

(b)

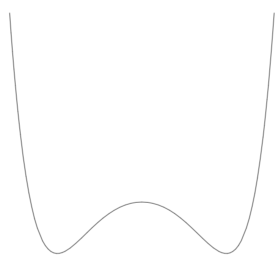

(c)

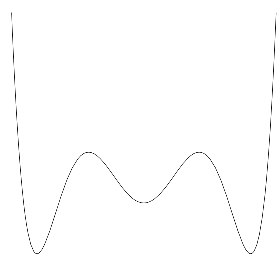

(d)

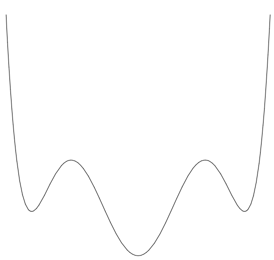

(e)

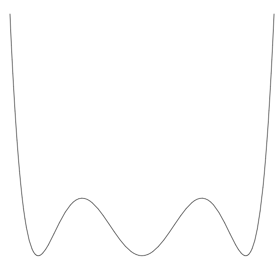

(f)

Figure 1.2: Phase diagram of the Ginzburg–Landau model (1.13). The blue and red lines mark the first- and second-order phase transitions, respectively. The green dashed line is $g_2 = g_4^2/3$.

1.3 Complex magnetic field

As I wrote in the introduction, the study of the Ising model in a complex magnetic field H was introduced by Yang and Lee in 1952. In their first paper [1] they studied the grand partition function of a lattice gas with complex fugacity y, proving that the equation of state can be deduced by the distribution of the singularities of the free energy F. The second paper [2] established the equivalence between the Ising model and a lattice gas with a suitable potential. In particular, the fugacity was found to be proportional to the exponential of the magnetic field:

$$y \propto e^{-2\beta H} . \tag{1.14}$$

Then a theorem was proved that, for a broad class of potentials (including the one corresponding to the Ising model), all the zeros of the grand partition function lie on the unit circle of the complex y-plane (equivalently, all the poles of the free energy are located on the imaginary axis of the complex H-plane).

For $\beta < \beta_c$ (high-temperature regime), the poles accumulate in the thermodynamic limit towards the points $H = \pm i H_0(\beta)$ with real $H_0 > 0$ (see Fig. 1.3). As accumulation points of poles, $\pm i H_0$ are essential singularities for the free energy: they are removed from the complex plane by drawing a cut along the imaginary axis. The cut passes through the point at infinity: the free energy is analytic for any real value of H because we know there is no phase transition. The gap in the distribution of the poles reduces while lowering the temperature, unless, at the critical point, it happens that $H_0(\beta_c) = 0$. Now it is no more possible to analytically continue $F(\beta, H)$ from positive to negative H: this is the signal of the phase transition. Fisher [13] named Yang–Lee edge singularities the points $\pm i H_0(\beta)$, and proved that the accumulation of zeros of the partition function in the thermodynamic limit is a conventional critical phenomenon, with scaling laws, universality and so on. In high dimension D, it corresponds to the infrared behaviour of the field theory with an action

$$\mathcal{A}_{YL} = \int d^D x \left[\frac{1}{2} (\partial_\mu \phi)^2 + i(h - h_0)\phi + i\gamma\phi^3 \right] . \tag{1.15}$$

Note that such a theory is nonunitary because of the imaginary couplings. The theory of Yang–Lee edge singularity was enriched by Cardy [14] who showed how it is related to the simplest nonunitary minimal model characterized by central charge $c = -22/5$. Both Fisher's and Cardy's arguments are reproduced in Sec. B.2.

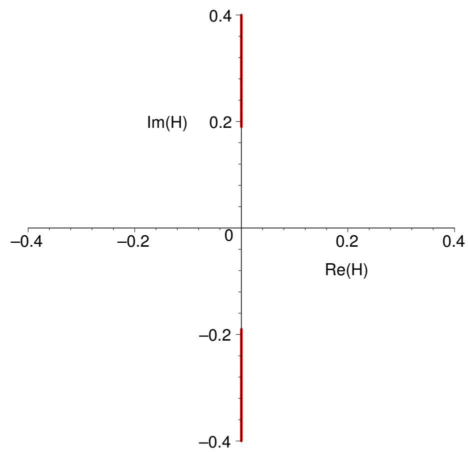

Figure 1.3: Ising model: branch cuts of the free energy in the complex H plane. The magnetic field is measured in units of $|2\pi g_2|^{15/8}$.

On the other hand, for $\beta > \beta_c$ (low-temperature regime), if one tries to continuously change the magnetic field from $H > 0$ to $H < 0$, at $H = 0$ one enters a metastable phase. Eventually the spinoidal singularity is reached, when the metastable phase holds no more and the state of the system change abruptly (see Fig. 1.4). In fact, the above picture must be corrected by taking into account thermic fluctuations [15]. They make the system start decaying through nucleation before reaching the spinoidal singularity. A cut (named Langer's branch cut) is therefore drawn along the negative H-axis (see Fig. 1.5), starting from $H = 0$ where is a weak singularity.

What happens to the spinoidal point when the Langer's branch cut is opened? Fonseca and Zamolodchikov answer that it is pushed under the cut in order to reappear in the high-temperature regime under the name of Yang–Lee edge singularity. This identification completes[1] the task of describing the analytical properties of the free energy in the complex magnetic field plane.

In order to support their claim, Fonseca and Zamolodchikov use the Ising field theory, formally defined by the action

$$\mathcal{A}_{IFT} = \mathcal{A}_{(c=1/2)} + g_1 \int \sigma(x) d^2x + g_2 \int \varepsilon(x) d^2x \, . \tag{1.16}$$

In the above formula $\mathcal{A}_{(c=1/2)}$ represents the action of the simplest unitary minimal model, $\sigma(x)$ and $\varepsilon(x)$ are the primary fields of the theory, that we can interpret as spin and thermal operators, while g_1 and g_2 are couplings related

[1] In fact, the comparison with lattice results (see Ref. [16]) could still hide some tricky point, as you know far better than me!

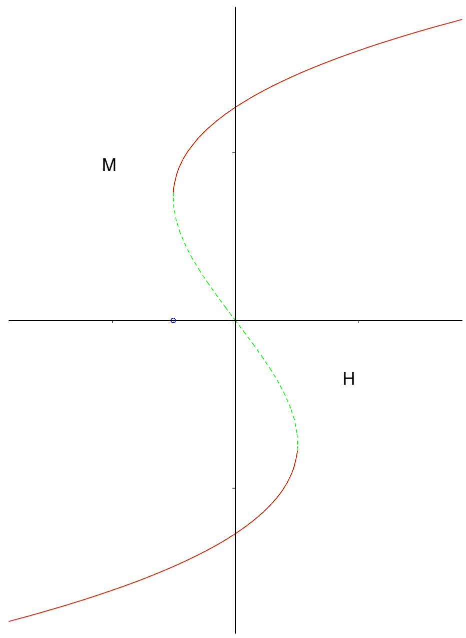

Figure 1.4: Magnetization versus the magnetic field for $\beta > \beta_c$: appearance of the spinoidal point.

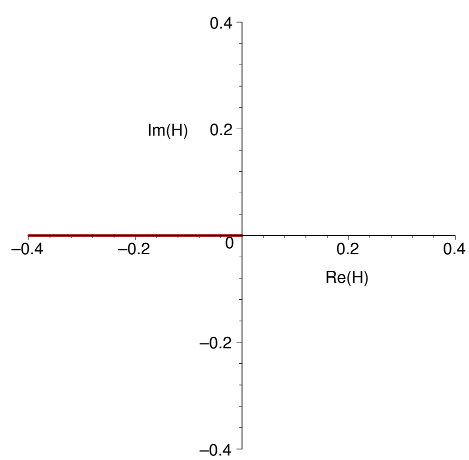

Figure 1.5: Low-temperature complex H-plane: the Langer's branch cut extends along the negative real axis

to departures from the critical point in the magnetic or in the temperature direction, respectively. Actually, it is possible to put together the first two terms on the RHS of Eq. (1.16) and substitute them with the free fermions action

$$\mathcal{A}_{FF} = \frac{1}{2\pi} \int \left[\psi \bar{\partial} \psi + \bar{\psi} \partial \bar{\psi} + i m \bar{\psi} \psi\right] d^2 x \,, \tag{1.17}$$

where $m = 2\pi g_2$, and $\psi, \bar{\psi}$ are the two chiral components of a Majorana field. Whichever formulation one employs, when the Ising field theory is put on a cylinder, its radius R acts as an infrared regulator, so that the spectrum is infrared finite. By means of a suitable truncation of the Hilbert space the problem of measuring the energy levels is reduced to the diagonalization of a finite dimensional Hamiltonian. One has access to the free energy by studying the infrared (that is, $R \to \infty$) behavior of the ground state.

1.4 Layout of the paper

The next chapter gives an extremely brief review of topics in conformal and integrable field theory. The relevant data about the tricritical Ising model and its various integrable and non-integrable deformations are summarized in Ch. 3. Finite size effects in conformal and integrable field theory are discussed in Ch. 4: this is a good introduction to the description of the computational technique here adopted, based on truncation of conformal space (in the following often abbreviated TCS), that is extensively described in Ch. 5. The outcome of my research is presented in Ch. 6, where the analytic structure of the free energy of the tricritical Ising model is numerically investigated. Two interesting byproducts of my analysis are also reported in the same chapter: some nice pictures of the evolution of the spectrum under renormalization group flows, and the numerical determination of some amplitudes useful for defining universal quantities. The last chapter is devoted to a summary of results and an outlook on possible future developments.

Chapter 2

Conformal and Integrable Field Theory

In this chapter some topics in quantum field theory that are relevant for this work are sketched. The first section provides a synthetic vocabulary of conformal field theory. Details and proofs and much more can be found in the textbook written by Di Francesco, Mathieu and Sénéchal [17]. Other classical references are the review paper by Ginsparg [18] or the book written by Itzykson and Drouffe [19].

Conformal field theory in two dimensions is characterized by an infinite number of conservation laws. Even in the presence of infinitely many conserved quantities, the task of solving the field theory (that is computing all correlation functions) is so tough that it can be completely carried on only for those particularly simple conformal field theories called minimal models (Sec. 2.2).

A part from their mathematical interest, minimal models are physically noteworth because they describe the scaling limit of discrete statistical models at their critical point. A second order phase transition is indeed characterized by the divergence of the correlation length: that is the reason why the physics of criticality results scale invariant, once the microscopical scale of the lattice details is eliminated by taking the scaling limit. Systems slightly off the critical point (see Ref. [20] for an extensive review) are described by suitable deformations of minimal models. Even if they breaks conformal invariance, some of these deformations inherit from the parent conformal field theory the nice feature of being subject to infinitely many conservation laws: the corresponding field theories are called integrable (Sec. 2.3). Some techniques peculiar to integrable field theories are mentioned in the last section: bootstrap approach for the S-matrix and form factors expansion. Another one, the thermodynamic Bethe Ansatz, is more extensively treated in Sec 4.2.

2.1 ABC of conformal field theory

Let us consider an Euclidean space of dimension D. The group of transformations $\mathbf{x} \to \mathbf{x}'$ that preserve the metric $g_{\mu\nu}$ up to a local rescaling:

$$g'_{\mu\nu}(\mathbf{x}') = \Lambda(\mathbf{x}) g_{\mu\nu}(\mathbf{x})\,, \tag{2.1}$$

is called conformal group. Its elements are generated by combinations of the following transformations:

$$x'^{\mu} = x^{\mu} + a^{\mu} \tag{2.2}$$

$$x'^{\mu} = M^{\mu}{}_{\nu} x^{\nu} \tag{2.3}$$

$$x'^{\mu} = \alpha x^{\mu} \tag{2.4}$$

$$x'^{\mu} = \frac{x^{\mu} - b^{\mu}\mathbf{x}^2}{1 - 2\mathbf{b}\cdot\mathbf{x} + \mathbf{b}^2\mathbf{x}^2}\,, \tag{2.5}$$

where $\mu, \nu = 1, \ldots, D$ and $\mathbf{b}\cdot\mathbf{x} = b^{\mu}x^{\nu}g_{\mu\nu}$. The first two are the familiar translation and rigid rotation, the third is a dilation, and the last takes the name of special conformal transformation. An element of the conformal group is therefore identified by $\frac{1}{2}(D+2)(D+1)$ real parameters (in fact the isomorphism with the group $\mathsf{SO}(D+1,1)$ can be proved).

In the case $D = 2$ the group of globally defined conformal transformations has 6 generators (in fact, it is $\mathsf{SL}(2,\mathbb{C})$), but any holomorphic (or antiholomorphic) mapping from the complex plane onto itself can be considered a local (in the sense that it is not necessarily defined everywhere) conformal transformation. This is easily seen by recognizing that Eq. (2.1) for $\mathbf{x} = (x^1, x^2)$ is equivalent to the Cauchy–Riemann equations. Hence the local symmetry group of a two-dimensional conformal field theory possesses infinitely many generators, that are the coefficients of the Laurent expansion of $\mathbf{x}'(\mathbf{x})$ around $\mathbf{x}$.

It is convenient to define complex variables

$$z = x^1 + ix^2 \qquad\qquad \bar{z} = x^1 - ix^2\,, \tag{2.6}$$

so that the holomorphic (antiholomorphic) Cauchy–Riemann equation is written simply

$$\partial_{\bar{z}} z'(z,\bar{z}) = 0 \qquad\qquad (\partial_z z'(z,\bar{z}) = 0)\,. \tag{2.7}$$

The fields $\phi(z,\bar{z})$ that under the conformal map $z \to w(z)$, $\bar{z} \to \bar{w}(\bar{z})$ transform as[1]

$$\phi'(w,\bar{w}) = \left(\frac{\partial w}{\partial z}\right)^{-h} \left(\frac{\partial \bar{w}}{\partial \bar{z}}\right)^{-\bar{h}} \phi(z,\bar{z}) \tag{2.8}$$

are called primary. The real numbers $(h,\bar{h})$ are called holomorphic and antiholomorphic conformal dimensions, $h+\bar{h}$ is called scaling dimension of the field and $h-\bar{h}$ is the spin.

A conformal field $\phi(z,\bar{z})$ of dimension $(h,\bar{h})$ may be mode expanded as follows:

$$\phi(z,\bar{z}) = \sum_{m\in\mathbb{Z}}\sum_{n\in\mathbb{Z}} z^{-m-h}\bar{z}^{-n-\bar{h}}\phi_{m,n}\,. \tag{2.9}$$

If we expand in such a way the holomorphic and antiholomorphic (also called left and right) components of the energy-momentum tensor, we get

$$T(z) = \sum_{n\in\mathbb{Z}} z^{-n-2}L_n \qquad \bar{T}(\bar{z}) = \sum_{n\in\mathbb{Z}} \bar{z}^{-n-2}\bar{L}_n\,, \tag{2.10}$$

where $T = -2\pi T_{zz}$ and $\bar{T} = -2\pi T_{\bar{z}\bar{z}}$. The coefficients $L_n, \bar{L}_n$ can be considered generators of the local conformal transformations on the Hilbert space. They obey the Virasoro algebra

$$\begin{aligned}
[L_n, L_m] &= (n-m)L_{n+m} + \frac{c}{12}n(n^2-1)\delta_{n+m,0} \\
[L_n, \bar{L}_m] &= 0 \\
[\bar{L}_n, \bar{L}_m] &= (n-m)\bar{L}_{n+m} + \frac{c}{12}n(n^2-1)\delta_{n+m,0}\,.
\end{aligned} \tag{2.11}$$

The central charge c classifies different conformal field theories and has the physical meaning of Casimir energy for the theory put on a cylinder (see Sec. 5.1).

2.2 Minimal models of conformal field theory

The minimal models [21] are characterized by a Hilbert space made of a finite number of representations of the Virasoro algebra (2.11). The first issue to be addressed is therefore to find irreducible representations of the Virasoro algebra, then we will be ready to give a very concise summary of minimal models' properties (a complete treatment of this subject can be found in Ref. [17]).

[1]Note that z and $\bar{z}$ are considered independent (this is the same as promoting x^1, x^2 to complex variables): the physical space can be recovered by selecting the real surface $\bar{z} = z^*$.

2.2.1 Irreducible representations of the Virasoro algebra

Since no pair of generators commute in the Virasoro algebra (2.11), only one of them (the usual choice is L_0) can be diagonalized in the representation space, often called Verma module. The highest-weight states $|h\rangle$ are thus labelled by the eigenvalues h of L_0

$$L_0|h\rangle = h|h\rangle\,. \tag{2.12}$$

The raising and lowering operators are all L_m with m negative or positive, respectively. The highest-weight states are therefore defined also by the condition

$$L_m|h\rangle = 0 \qquad \forall m > 0\,. \tag{2.13}$$

A basis for the descendant states is obtained by applying the raising operator in all possible ways:

$$L_{-k_1}L_{-k_2}\dots L_{-k_n}|h\rangle \qquad 1 \leq k_1 \leq k_2 \leq \cdots \leq k_n \tag{2.14}$$

is an eigenstate of L_0 with eigenvalue

$$h' = h + k_1 + k_2 + \cdots + k_n \equiv h + N\,, \tag{2.15}$$

where N is called the level of the state. The fourth level, for example, is the space spanned by the vectors

$$L_{-1}^4|h\rangle \quad L_{-1}^2L_{-2}|h\rangle \quad L_{-1}L_{-3}|h\rangle \quad L_{-2}^2|h\rangle \quad L_{-4}|h\rangle\,. \tag{2.16}$$

The Hermitian conjugation is defined by $L_m^\dagger = L_{-m}$, hence the inner product between two elements

$$L_{-k_1}\dots L_{-k_m}|h\rangle \qquad L_{-l_1}\dots L_{-l_n}|h\rangle \tag{2.17}$$

belonging to the same Verma module $V(c,h)$ is simply defined by

$$\langle h|L_{k_m}\dots L_{k_1}L_{-l_1}\dots L_{-l_n}|h\rangle\,. \tag{2.18}$$

The Verma modules associated with the antiholomorphic generators $\bar{L}_m$ are built in the same way. The complete Hilbert space $\mathfrak{H}$ is in general a direct sum over all conformal dimensions of tensor products of Verma modules

$$\mathfrak{H} = \bigoplus_{h,\bar{h}} V(c,h) \otimes \bar{V}(c,\bar{h})\,. \tag{2.19}$$

To a Verma module $V(c,h)$ it is possible to associate a generating function $\chi_{(c,h)}(q)$ called the character of the module, whose definition is

$$\chi_{(c,h)}(q) = \mathrm{Tr}\, q^{L_0 - c/24} = \sum_{n=0}^{\infty} \dim(h+n) q^{n+h-c/24}\,, \tag{2.20}$$

where q is a complex variable, and $\dim(h+n)$ is the number of linearly independent states at level n in the Verma module. Each Verma module is a representation of the Virasoro algebra. In order to obtain an irreducible representation, one must quotient out the vectors $|\chi\rangle$ such that $\langle\chi|\chi\rangle = 0$. These are called null vectors. The irreducible representations of the Virasoro algebra are the building blocks of the minimal models.

2.2.2 Unitary and nonunitary minimal models

Any highest-weight state $|h,\bar{h}\rangle$ can also be seen as an asymptotic (that is, in the context of radial quantization, $z, \bar{z} \to 0$) state generated by a primary field $\phi(z,\bar{z})$ of conformal dimensions $(h,\bar{h})$ acting on the vacuum:

$$\phi(0,0)|0\rangle = |h,\bar{h}\rangle\,, \tag{2.21}$$

where the vacuum is defined by the property

$$L_n|0\rangle = 0 \qquad \bar{L}_n|0\rangle = 0 \qquad \forall n \leq -1\,. \tag{2.22}$$

As a space of descendant states can be built upon an highest-weight vector, so a family of descendant fields can be obtained by repeatedly applying suitable differential operators. The set comprising a primary field and all of its descendants is called conformal family. A conformal family is closed under conformal transformations.

An operator algebra between conformal families can be defined by taking the short-distance product of their primary fields: this is just another way of expressing the constraints that the conformal invariance dictates on the three-point correlation functions. The minimal models are those conformal field theories whose operator algebra truncates on a finite set of conformal families. They are completely classified by a pair of positive coprime integers (p,p') such that $p > p'$. We will thus indicate with $\mathcal{M}(p,p')$ the conformal field theory whose central charge is

$$c = 1 - 6\frac{p-p'}{pp'}\,, \tag{2.23}$$

and whose Kac table (containing the allowed conformal dimensions) is

$$h_{r,s} = \frac{(pr - p's)^2 - (p - p')^2}{4pp'}\,, \tag{2.24}$$

where

$$1 \le r < p' \qquad\qquad 1 \le s < p\,. \tag{2.25}$$

An explicit formula can be given for the Virasoro character $\chi_{c,h_{r,s}}(q)$ [22]:

$$\chi_{(c,h_{r,s})}(q) = \frac{q^{h+(1-c)/24}}{\eta(q)} \sum_{k=-\infty}^{\infty} q^{-pp'k^2}\left(q^{k(pr-p's)} - q^{k(pr+p's)}\right) \tag{2.26}$$

in terms of the Dedekind function

$$\eta(q) \equiv q^{1/24} \prod_{n=1}^{\infty} (1 - q^n)\,. \tag{2.27}$$

A representation of the Virasoro algebra is said to be unitary if it contains no negative-norm states. It turns out that a necessary condition for the unitarity of a Verma module with highest weight h is $h \ge 0$. Therefore we call unitary the minimal models whose Kac table contains only non-negative conformal dimensions. These are characterized by the condition $p = 1 + p'$. The first such non-trivial model is $\mathcal{M}(4,3)$, which describes the class of universality of the critical point in the Ising model. The next one, $\mathcal{M}(5,4)$ is the tricritical Ising model. On the other hand, the simplest non-unitary minimal model is $\mathcal{M}(5,2)$, that is related to the description of the Yang–Lee edge singularity.

2.2.3 Operator content of a minimal model

A relevant property of the Virasoro algebra Eq. (2.11) is that holomorphic and antiholomorphic generators are completely independent. It could seem that, in the sum Eq. (2.19) defining the Hilbert space of the theory, we are free to combine any $V(c,h)$ with any other $\bar{V}(c,\bar{h})$. In fact, we expect that only few choices would be physically sensible: the reason is that the decoupling of left and right modes is destroyed as we move off the critical point, but on the other hand the spectrum should change continuously. It turns out that the easiest way to relate left and right components is by changing the topology of the space where the critical theory is defined, rather than facing the intricacies of the off-critical theory.

The complex plane is topologically equivalent to a sphere: if we are looking for constraints on the left-right coupling, we need to consider at least a torus. In the operator formalism the main role is played by the partition function [23]

$$Z(q) = \mathrm{Tr}\left(q^{L_0-c/24}\bar{q}^{\bar{L}_0-c/24}\right), \tag{2.28}$$

where q is exactly the same parameter used in writing Eq. (2.20) and is related to the modular parameter τ of the torus[2] by the relation $q = \exp(2\pi i\tau)$. The request of modular invariance for the partition function severely constraints the operator content of minimal models: a complete classification was carried over when the one-to-one correspondence between the modular invariant partition functions of the minimal model $\mathcal{M}(p,p')$ and the pairs of simply laced Lie algebras $(A_n, D_n, E_6, E_7, E_8)$ with respective dual Coxeter numbers p' and p was conjectured [24] and subsequently proved [25, 26].

2.3 Integrable field theory

A field theory for which we can establish infinitely many conservation laws is said to be integrable. Any conformal field theory in two dimensions is integrable, because of the infinite dimensionality of the group of local conformal transformations. Other integrable field theories can be obtained by suitable deformations of minimal models.

2.3.1 Conserved quantities

In two-dimensional quantum field theory a conservation law takes the form

$$\partial_{\bar{z}} T_{s+1}(z,\bar{z}) = \partial_z \Theta_{s-1}(z,\bar{z}), \tag{2.29}$$

where T_{s+1} and Θ_{s-1} are local operators with spin $s+1$ and $s-1$, respectively. The corresponding conserved charge has the form

$$\mathcal{C}_s = \int \left(T_{s+1}dz - \Theta_{s-1}d\bar{z}\right). \tag{2.30}$$

In the particular case $s = 1$, T_2 is the holomorphic component and Θ_0 is one fourth of the trace of the energy-momentum tensor. A part from this, that is common to all field theories, for some theory it is possible to find other conservation laws. The so-called "counting argument" suggested by Alexander Zamolodchikov [27, 28] permits to check when this can be done.

Let us consider a theory formally defined by the action

$$\mathcal{A} = \mathcal{A}_{CFT} + g\int d^2x\, \phi(x), \tag{2.31}$$

[2]The torus is defined as the complex plane modulo τ, where τ is a complex number.

that is a conformal action perturbed by a relevant ($h < 1$) operator. A conservation law like Eq. (2.29) can be found if the dimension of the space of descendants of the identity operators at level $s+1$ is greater than the dimension of the space of descendants of the perturbing field at level $s-1$. Such a condition is promptly checked by using the character formula Eq. (2.26).

2.3.2 Exact S-matrix

When perturbed in the sense of Eq. (2.31), a conformal field theory in general develops a finite correlation length λ, so therefore it admits a description in terms of one or more particles of mass greater or equal to $m \propto 1/\lambda$. As it is natural to expect, the presence of an infinite number of conserved quantities[3] severely constraints the possible form of the S-matrix, ultimately permitting its exact (that is, non-perturbative in the interaction) determination. The scattering process of an integrable field theory is indeed characterized by the properties of elasticity and factorization. Elasticity means that the final set of energies and momenta coincides with the initial one: in particular, there is no particle production. Factorization means that any n-particle scattering amplitude factorizes into the product of $n(n-1)/2$ two-particle amplitudes. Factorization is algebraically expressed under the form of Yang–Baxter equations.

These two simplifications, together with the fact that in $1+1$ dimensions the particles move on a line, so there are no scattering angles, are powerful enough to derive the S-matrix from few fundamental principles: unitarity, crossing symmetry, and the assumption of maximal analiticity. This last point means that the two-particle S-matrix is an analytic function of the Mandelstam variable that possesses only those poles which are of physical origin (i.e. those that signal the occurrence of a bound state). The only model-dependent input is the assumption of a particle spectrum. The process of building the whole spectrum from "guessing" the scattering amplitudes of the lightest particles is called "bootstrap" (a recent review on the bootstrap program may be found in Ref. [30]).

2.3.3 Correlation functions

Finding the S-matrix is a noteworth achievement, but the real stake are the correlation functions. In integrable field theory they can be computed by

[3]In fact, the existence of just one conservation law besides the trivial one with $s = 1$ is sufficient to grant the elasticity and factorization properties [29].

means of an expansion in terms of the matrix elements between multiparticle states, called form factors. It is convenient to parameterize the on-shell momentum in terms of the rapidity variable θ defined by

$$(p^0, p^1) \equiv (m \cosh\theta, m \sinh\theta)\,, \tag{2.32}$$

where m is the mass. With this convention, the form factors for an operator ϕ are defined by

$$F^{\phi}_{a1\ldots a_n}(\theta_1, \ldots, \theta_n) = \langle 0|\phi(0)|A_{a_1}(\theta_1)\ldots A_{a_n}(\theta_n)\rangle\,, \tag{2.33}$$

where $|0\rangle$ is the vacuum and $A_{a_i}(\theta_i)$ is the creation operator for a particle of type a_i and rapidity θ_i. Now any correlation function can be expressed as a sum over form factors: for example, consider the two-point function

$$\langle\phi_1(x)\phi_2(0)\rangle\ : \tag{2.34}$$

by inserting the resolution of the identity

$$\mathbb{I} = \sum_{n=0}^{\infty} \frac{1}{(2\pi)^n} \int_{\theta_1 > \cdots > \theta_n} d\theta_1 \ldots d\theta_n |A_{a_1}(\theta_1)\ldots A_{a_n}(\theta_n)\rangle\langle A_{a_n}(\theta_n)\ldots A_{a_1}(\theta_1)| \tag{2.35}$$

it can be expressed in terms of form factors

$$\langle\phi_1(x)\phi_2(0)\rangle = \sum_{n=0}^{\infty} \frac{1}{(2\pi)^n} \int_{\theta_1 > \ldots \theta_n} d\theta_1 \ldots d\theta_n F^{\phi_1}_{a_1\ldots a_n}(\theta_1 \ldots \theta_n) \left[F^{\phi_2}_{a_1\ldots a_n}(\theta_1 \ldots \theta_n)\right]^* e^{-|x|E_n} \tag{2.36}$$

where

$$E_n = \sum_{k=1}^{n} m_{a_k} \cosh\theta_k\,. \tag{2.37}$$

The properties characterizing the scattering processes in integrable field theories can be translated into five equations for the form factors [31]: these equations can be solved[4]. What is not in general possible is to sum the series and exactly compute the correlation function. However, Eq. (2.36) can be considered a long distance ($|x| \gg \lambda$) expansion, indeed a very effective one because the first few terms usually give a good approximation. The data from form factor expansion is complemented by a short distance expansion obtained by perturbing around the conformal point [33]. By using both expansions, many correlations functions in integrable models can be computed with good accuracy.

[4]The trick called "asymptotic factorization" [32] will in general be needed in order to distinguish the form factors of different fields.

Chapter 3

Tricritical Ising model

The class of universality of tricritical points occurring in two-dimensional statistical models whose order parameter enjoys $\mathbb{Z}_2$ symmetry, for instance the Blume–Emery–Griffiths model introduced in Sec. 1.1, is described (in the scaling limit) by the minimal conformal field theory characterized by central charge $c = 7/10$. Due to its various infinite-dimensional symmetries, the TIM has been defined "a theorist's ideal playground" [34]. All data about this minimal model and its deformations relevant for my thesis are collected in this chapter.

3.1 The minimal model $\mathcal{M}(5,4)$

The Kac table of the minimal model $\mathcal{M}(5,4)$, as obtained from Eq. (2.24), is given in Tab. 3.1. In the framework of radial quantization, it is natural to define the theory on a cylinder by means of the conformal mapping $w = \frac{R}{2\pi} \ln \frac{z}{R}$ (see Sec. 5.1). The operator content of the theory depends on the choice of boundary conditions [34] on the coordinate $u = \Re(w)$.

For periodic boundary conditions, the modular invariant partition function is diagonal. The corresponding operator content is summarized in

0	$\frac{1}{10}$	$\frac{3}{5}$	$\frac{3}{2}$
$\frac{7}{16}$	$\frac{3}{80}$	$\frac{3}{80}$	$\frac{7}{16}$
$\frac{3}{2}$	$\frac{3}{5}$	$\frac{1}{10}$	0

Table 3.1: Kac table of the minimal model $\mathcal{M}(5,4)$

$(0,0)$	$\mathbb{I}$		identity	
$(\frac{3}{80},\frac{3}{80})$	σ	φ_1	magnetization	Φ
$(\frac{1}{10},\frac{1}{10})$	ε	φ_2	energy	$:\Phi^2:$
$(\frac{7}{16},\frac{7}{16})$	σ'	φ_3	submagnetization	$:\Phi^3:$
$(\frac{3}{5},\frac{3}{5})$	t	φ_4	chemical potential	$:\Phi^4:$
$(\frac{3}{2},\frac{3}{2})$	ε''		(irrelevant)	$:\Phi^6:$

Table 3.2: Operators in the TIM with periodic boundary conditions

Tab. 3.2: in the first column there are the conformal dimensions, the second and third columns report the symbols I will use in referring to these fields, while the fourth contains a concise description of their physical meaning. The rightmost column shows the correspondence [35] with the normal ordered fields of the Landau–Ginzburg formulation. Fusion rules and structure constants of the operator algebra can be computed in the framework of the Coulomb gas formalism [36, 37]: the result is summarized in Tab. 3.3.

If the boundary conditions on the u-direction are $\mathbb{Z}_2$-twisted, on the other hand, the partition function is not diagonal: the operator content of the theory is displayed in Tab. 3.4, while the non-trivial fusion rules can be found in Tab. 3.5.

The tricritical Ising model exhibits several discrete as well as continuous symmetries. First of all, there is the $\mathbb{Z}_2$ symmetry related to the spin-reversal transformation, that in the Landau–Ginzburg approach corresponds to $\Phi \to -\Phi$. The fields $\mathbb{I}, \varepsilon, t, \varepsilon''$ are even with respect to such a transformation, while σ, σ' are odd. An inspection of the fusion rules shows that the even operators form a subalgebra.

Another symmetry mutuated from the lattice model is the Kramers–Wannier duality, under which the magnetization operators σ, σ' are mapped onto their corresponding disorder operators μ, μ', while $\varepsilon, \varepsilon''$ are odd, and t is even. The behavior of primary operators of TIM under these two discrete symmetries is summarized in Tab. 3.6.

The tricritical Ising model can also be realized in terms of a coset construction of a Wess–Zumino–Witten model on the group

$$\frac{(\mathsf{E}_7)_1 \otimes (\mathsf{E}_7)_1}{(\mathsf{E}_7)_2}\,. \tag{3.1}$$

(see Ref. [38] where this property is exploited for the computation of the even × even

$$\varepsilon \times \varepsilon = [[\mathbb{I}]] + c\,[[t]] \qquad t \times t = [[\mathbb{I}]] + c\,[[t]]$$

$$\varepsilon \times t = c\,[[\varepsilon]] + \frac{3}{7}\,[[\varepsilon'']] \qquad \varepsilon'' \times \varepsilon'' = [[\mathbb{I}]]$$

even × odd

$$\varepsilon \times \sigma = \frac{1}{2}\,[[\sigma']] + \frac{3}{2}c\,[[\sigma]] \qquad \varepsilon \times \sigma' = \frac{1}{2}\,[[\sigma]]$$

$$t \times \sigma = \frac{3}{4}\,[[\sigma']] + \frac{1}{4}c\,[[\sigma]] \qquad t \times \sigma' = \frac{3}{4}\,[[\sigma]]$$

odd × odd

$$\sigma' \times \sigma' = [[\mathbb{I}]] + \frac{7}{8}\,[[\varepsilon'']] \qquad \sigma' \times \sigma = \frac{1}{2}\,[[\varepsilon]] + \frac{3}{4}\,[[t]]$$

$$\sigma \times \sigma = [[\mathbb{I}]] + \frac{3}{2}c\,[[\varepsilon]] + \frac{1}{4}c\,[[t]] + \frac{1}{56}\,[[\varepsilon'']]$$

$$c = \frac{2}{3}\sqrt{\frac{\Gamma(4/5)\Gamma^3(2/5)}{\Gamma(1/5)\Gamma^3(3/5)}}$$

Table 3.3: Fusion rules and structure constants for TIM: periodic boundary conditions

$(\frac{3}{80}, \frac{3}{80})$	μ	disorder field
$(\frac{7}{16}, \frac{7}{16})$	μ'	subleading disorder field
$(\frac{3}{5}, \frac{1}{10})$	ψ	fermion
$(\frac{1}{10}, \frac{3}{5})$	$\bar{\psi}$	anti-fermion
$(\frac{3}{2}, 0)$	G	SuSy generator
$(0, \frac{3}{2})$	$\bar{G}$	SuSy generator

Table 3.4: Operators in the TIM with $\mathbb{Z}_2$-twisted boundary conditions

$$\psi \times \psi = \bar{\psi} \times \bar{\psi} = [[\mathbb{I}]] + c\,[[t]] \qquad \psi \times \bar{\psi} = -\bar{\psi} \times \psi = ic\,[[\varepsilon]] + i\frac{3}{7}\,[[\varepsilon'']]$$

$$\psi \times G = -\bar{G} \times \bar{\psi} = i\frac{3}{7}\,[[\varepsilon]]$$

$$c = \frac{2}{3}\sqrt{\frac{\Gamma(4/5)\Gamma^3(2/5)}{\Gamma(1/5)\Gamma^3(3/5)}}$$

Table 3.5: Fusion rules and structure constants for TIM: $\mathbb{Z}_2$-twisted boundary conditions

field	spin-reversal	Kramers–Wannier
ε	ε	$-\varepsilon$
t	t	t
ε''	ε''	$-\varepsilon''$
σ	$-\sigma$	μ
σ'	$-\sigma'$	μ'

Table 3.6: Discrete symmetries of TIM

matrix elements of the energy-momentum tensor as well as of its two-point correlation function).

The tricritical Ising model is also the simplest example of superconformal field theory [39]: its Hilbert space contains a finite number of irreducible representations of the super-Virasoro algebra (the antiholomorphic part is omitted)

$$[L_m, L_n] = (m-n)L_{m+n} + \frac{c}{12}(m^3 - m)\delta_{m,-n} \tag{3.2}$$

$$\{G_m, G_n\} = 2L_{m+n} + \frac{c}{3}\left(m^2 - \frac{1}{4}\right)\delta_{m,-n} \tag{3.3}$$

$$[L_m, G_n] = \left(\frac{1}{2}m - n\right) G_{m+n} \,. \tag{3.4}$$

As the generators L_n arise as coefficients in the expansion of the energy-momentum tensor, so the G_n are Fourier components of the superpartner of the energy-momentum tensor, the field $G(z)$ with conformal dimensions $(3/2, 0)$. The theory is splitted into two sectors depending on the boundary conditions imposed on the $\Im(w)$ direction: in the Neveu–Schwarz sector the even fields can be grouped into a superfield

$$\mathcal{N}(z, \bar{z}, \theta, \bar{\theta}) = \varepsilon(z, \bar{z}) + \bar{\theta}\psi(z, \bar{z}) + \theta\bar{\psi}(z, \bar{z}) + \theta\bar{\theta}t(z, \bar{z}) \,, \tag{3.5}$$

where $\theta, \bar{\theta}$ are Grassman variables; in the Ramond sector the magnetic fields give rise to two irreducible representations.

3.2 Off-critical behaviour

This section contains a brief summary of what happens when we depart from the fixed point along one of the four relevant directions. The perturbed theories are formally defined by the actions

$$\mathcal{A}_i = \mathcal{A}_{(c=7/10)} + g_i \int d^2x \, \varphi_i(x) \qquad i = 1, \ldots, 4 \,, \tag{3.6}$$

where g_i can be either positive or negative. Since φ_1 and φ_3 are odd under spin-reversal transformation, a change of the sign of g_1 or g_3 has no effect on the spectrum: we will simply write $\mathcal{A}_1$ or $\mathcal{A}_3$. In a similar way, φ_2 is even with respect to the spin-reversal transformation, but odd under Kramers–Wannier duality, hence $\mathcal{A}_2^+$ and $\mathcal{A}_2^-$ are dual descriptions of the high- and low-temperature regimes of the same theory. Only φ_4 is even with respect to both the $\mathbb{Z}_2$ symmetries of TIM: as a consequence, $\mathcal{A}_4^+$ and $\mathcal{A}_4^-$ represent two

$\mathcal{A}_1$	$\mathcal{A}_2^+$	$\mathcal{A}_2^-$	$\mathcal{A}_3$	$\mathcal{A}_4^+$	$\mathcal{A}_4^-$
nonintegr. 3 masses	integr. E_7 high-temp.	integr. E_7 low-temp.	integr. kinks	integr. massless	integr. SuSy kinks

Table 3.7: Properties of QFTs obtained by deformation of tricritical Ising model

physically distinct theories. A quick reference to the main features of these theories is provided by Table 3.7.

The off-critical behavior of the tricritical Ising model is described in great detail in Ref. [34, 40], from which I borrow all the following data.

3.2.1 Leading magnetic perturbation

The perturbation by the field $\varphi_1 \equiv \sigma$ breaks all the symmetries of the conformal theory. For this deformation, Zamolodchikov's counting argument doesn't suggest integrability, moreover a TCS analysis shows that lines repel each other in the crossover region [34]: for these reasons we are reasonably confident that the off-critical behavior is not integrable. Because of the lack of integrability, a numerical approach like the truncation of conformal space (to be introduced in the next chapter) is the only source of data about this theory.

The spectrum contains three stable masses below threshold:

$$m_1 \qquad m_2 = 1.6(2)m_1 \qquad m_3 = 1.9(8)m_1 \,, \tag{3.7}$$

where the digit between round brackets is affected by error. The relation between the fundamental mass and the coupling constant g_1 has been estimated to be

$$m_1 \approx 3.242\ldots g_1^{40/77} \,. \tag{3.8}$$

3.2.2 Leading energy perturbation

The perturbation by $\varphi_2 \equiv \varepsilon$ with positive coupling constant drives the system into its high-temperature phase. The off-critical theory is integrable and related to the Toda field theory based on the exceptional algebra E_7: the conserved currents have spins

$$s = 1, 5, 7, 9, 11, 13, 17 \quad (\text{mod } 18) \,, \tag{3.9}$$

m_1	1	odd
$m_2 = 2m_1 \cos(5\pi/18)$	1.2856...	even
$m_3 = 2m_1 \cos(\pi/9)$	1.8794...	odd
$m_4 = 2m_1 \cos(\pi/18)$	1.9696...	even
$m_5 = 4m_1 \cos(\pi/18)\cos(5\pi/18)$	2.5321...	even
$m_6 = 4m_1 \cos(2\pi/9)\cos(\pi/9)$	2.8794...	odd
$m_7 = 4m_1 \cos(\pi/18)\cos(\pi/9)$	3.7017...	even

Table 3.8: Spectrum of the theory $\mathcal{A}_2^+$

(these numbers are the Coxeter exponents of the exceptional algebra E_7) and the spectrum is given in Tab. 3.8. The S-matrix, as well as the particle masses, is known exactly [41, 42] The relationship between the mass gap and the coupling constant can be exactly computed [43]:

$$\begin{aligned} m_1 &= \left(\frac{2\Gamma(\frac{2}{9})}{\Gamma(\frac{2}{3})\Gamma(\frac{5}{9})}\right)\left(\frac{4\pi^2\Gamma(\frac{2}{5})\Gamma^3(\frac{4}{5})}{\Gamma^3(\frac{1}{5})\Gamma(\frac{3}{5})}\right)^{5/18} |g_2|^{5/9} \\ &= |g_2|^{5/9} 3.7453728362\ldots. \end{aligned} \tag{3.10}$$

Since this theory is integrable, one can exploit the form factor expansion in order to compute correlation functions. However, as observed in Ref. [40], an obstacle occurs that drastically reduces the precision one can achieve by this technique: the asymptotic factorization argument [32] fails to discriminate between the form factors of φ_1 and those of φ_3. The one-particle form factors have therefore to be determined by some independent way, like the truncation of conformal space to be introduced in the next chapter. The low degree of precision in the determination of the one-particle form factors is the main obstacle to the evaluation of the three-particle ones.

3.2.3 Subleading magnetic perturbation

Also the perturbation by the field φ_3 is integrable [44]. The presence of two degenerate (and asymmetrical) vacua permits the existence of two massive kink excitations and one breather bound state, all with the same mass. The S-matrix is exactly known [45], as well as the relationship between the mass gap and the coupling constant:

$$\begin{aligned} m_1 &= \frac{\sqrt{3}\Gamma(\frac{1}{3})\Gamma(\frac{5}{9})}{\pi\Gamma(\frac{8}{9})}\left[\frac{\pi^2\Gamma(\frac{1}{4})\Gamma^2(\frac{11}{16})}{\Gamma(\frac{3}{4})\Gamma^2(\frac{5}{16})}\right]^{4/9} g_3^{8/9} \\ &= g_3^{8/9} 4.92779064\ldots. \end{aligned} \tag{3.11}$$

3.2.4 Subleading energy perturbation

The deformation by the field φ_4 is related to the change in the vacancy density: if we move in the direction $g_4 > 0$, then we are increasing the number of spins that take values ± 1, while in the direction $g_4 < 0$ the spins taking value 0 are favored. Both the theories are integrable [46]. The $g_4 > 0$ deformation originates a massless renormalization group flow [47] at the ending point of which there is the Ising field theory $\mathcal{M}(4,3)$. Along this flow, the conformal dimension of the magnetization operator changes from the value $\frac{3}{80}$ to $\frac{1}{16}$, while the conformal dimension of the energy operator changes from $\frac{1}{10}$ to $\frac{1}{2}$. The exact massless S-matrix [48] and form factors [49] for the theory $\mathcal{A}_4^+$ are available. If $g_4 < 0$, on the other hand, the corresponding Landau–Ginzburg potential is threefold degenerate: the elementary excitations are massive kinks [46]. The scattering theory is considered in Ref. [50].

Chapter 4

Finite size effects

In this chapter two ingredients of the truncation of conformal space recipe, to be treated in the next chapter, are introduced: the Hamiltonian formalism of CFT and the dependence of the Hamiltonian's ground state on the compact dimension of the cylinder where the theory is defined.

4.1 Transfer matrix and Hamiltonian formalism

In order to motivate the introduction of Hamiltonian formalism in conformal field theory, let us take one step back to the lattice definition of a statistical spin system like the Ising or the Blume–Emery–Griffiths models defined in Sec. 1.1. To focus the ideas, let us consider the case of the Ising model defined on a square lattice of lattice spacing ℓ, with M rows and N columns. Any spin variable is identified by a pair of integers: $s_{m,n}$. Moreover, let us fix periodic boundary conditions $s_{M+1,n} = s_{1,n}$ and $s_{m,N+1} = s_{m,1}$. With such boundary conditions, the model is defined over a torus of dimensions $R = N\ell$ and $L = M\ell$. An efficent way to compute the partition function is splitting the configuration energy Eq. (1.1) into a term that represents the energy of the m-th row

$$E_m^{\text{row}} = -J \sum_{n=1}^{N} s_{m,n} s_{m,n+1} - H \sum_{n=1}^{N} s_{m,n} \,, \tag{4.1}$$

and a term that accounts for the interaction amongst different rows

$$E_{m,m+1}^{\text{int}} = -J \sum_{n=1}^{N} s_{m,n} s_{m+1,n} \,, \tag{4.2}$$

so that the total energy associated to a given spin configuration is

$$E_{\{s\}} = \sum_{m=1}^{M} (E_m^{\rm row} + E_{m,m+1}^{\rm int}) \,. \tag{4.3}$$

Let us associate to the configuration of spins in the m-th row a ket symbol

$$|\mu_m\rangle \equiv \{s_{m,1}, s_{m,2}, \dots, s_{m,N}\} \,. \tag{4.4}$$

In the 2^N-dimensional vector space of row configurations, the transfer matrix is formally defined by giving its matrix elements:

$$\langle \mu_m | \mathcal{T} | \mu_{m+1} \rangle = \exp\left[-\beta \left(E_{m,m+1}^{\rm int} + \frac{1}{2} E_m^{\rm row} + \frac{1}{2} E_{m+1}^{\rm row} \right) \right] \,, \tag{4.5}$$

in such a way that the partition function Eq. (1.2) takes the following simple form:

$$\begin{aligned} Z &= \sum_{\mu_1,\dots,\mu_M} \langle \mu_1 | \mathcal{T} | \mu_2 \rangle \langle \mu_2 | \mathcal{T} | \mu_3 \rangle \dots \langle \mu_M | \mathcal{T} | \mu_1 \rangle \\ &= {\rm Tr}\, \mathcal{T}^M = \sum_{k=0}^{2^N-1} \Lambda_k^M \,. \end{aligned} \tag{4.6}$$

The last equation is justified by the fact that the transfer matrix is manifestly symmetric, and therefore diagonalizable. The behavior of the free energy per spin, defined in Eq. (1.3), is dominated by the largest eigenvalues of $\mathcal{T}$:

$$\begin{aligned} -\beta F &= \lim_{M,N\to\infty} \frac{1}{MN} \ln(\Lambda_0^M + \Lambda_1^M + \dots) \\ &= \lim_{M,N\to\infty} \frac{1}{MN} \left[\ln(\Lambda_0^M) + \ln(1 + (\Lambda_1/\Lambda_0)^M + \dots) \right] \\ &= \lim_{M,N\to\infty} \left\{ \frac{1}{N} \ln\Lambda_0 + \frac{1}{MN} \exp\left(-M \ln\frac{\Lambda_0}{\Lambda_1} \right) + \dots \right\} \,, \end{aligned} \tag{4.7}$$

where $\Lambda_0 > \Lambda_1 > \Lambda_2 > \dots$.

If we identify a row with the 'space' and the transverse direction with the 'time', we can interpret the transfer matrix as an evolution operator

$$\mathcal{T} = \exp\left(-\ell \hat{H}_R \right) \,, \tag{4.8}$$

where $\hat{H}_R$ is the Hamiltonian operator on the circumference. The eigenvalues of $\mathcal{T}$ are equivalent to the energy levels $E_k(R)$ of $\hat{H}_R$,

$$E_k(R) = -\frac{1}{\ell} \ln\Lambda_k \,. \tag{4.9}$$

By using Eq. (4.9) in Eq. (4.7) we find for the free energy density

$$\begin{aligned}\frac{\beta F}{\ell^2} &= \lim_{L,R\to\infty}\left\{\frac{E_0(R)}{R} - \frac{1}{RL}\exp\{-L[E_1(R)-E_0(R)]\} + \dots\right\} \\ &\simeq \lim_{R\to\infty}\frac{E_0(R)}{R}\,.\end{aligned} \tag{4.10}$$

A suitable Hamiltonian for studying the free energy of the tricritical Ising model will be shown in Sec. 5.1.

4.2 Thermodynamic Bethe Ansatz

We have already seen in Sec. 2.3 some powerful tools that can be applied only to the study of integrable field theories. Another technique for getting non-perturbative results goes under the name of thermodynamic Bethe Ansatz. It was introduced by Alexei Zamolodchikov [51] as a relativistic generalization of a method originally employed by Yang [52].

The basic idea is quite simple: put a $\mathcal{N}$-particle system on a circle of length L. The particles may belong to different species, labelled by the index a. We assign the label $a = 1$ to the particle species characterized by the lowest mass. When particles are far apart, that is $|x_{i_k} - x_{i_{k+1}}| \gg 1/m_1$, the state of the system can be described by the wave function

$$\psi(x_{i_1}, x_{i_2}, \dots, x_{i_\mathcal{N}}) = \prod_{k=1}^{\mathcal{N}} \exp(ip_{i_k} x_{i_k})\,, \tag{4.11}$$

where relativistic effects are neglected and an ordering of the particles according to their coordinates is assumed:

$$x_{i_1} \ll x_{i_2} \ll \dots \ll x_{i_\mathcal{N}}\,. \tag{4.12}$$

If the theory is integrable, then the only effect of interaction can be an interchanging of two particle positions accompanied by a phase-shift:

$$S_{ab}(\theta_a - \theta_b) = \exp(i\sigma_{ab}(\theta_a - \theta_b))\,. \tag{4.13}$$

For the diagonal S-matrix, the unitarity[1] condition implies $S^2_{aa}(0) = 1$. If $S_{aa}(0) = -1$, then the wave function should be antisymmetric under the exchange of two particles with the same rapidity: this is not compatible with

[1] This is the unitarity of the S-matrix, not to be confused with the unitarity of the conformal field theory.

the Bose statistics, hence we have a selection rule saying that each value of rapidity can be occupied by at most one particle. This rule is obviously absent if the particles are fermions. If $S_{aa}(0) = 1$, then the exclusion rule applies to fermions but not to bosons. In the context of thermodynamic Bethe Ansatz, we will distinguish a 'fermionic' and a 'bosonic' behavior by the presence or absence, respectively, of a selection rule on the rapidities: this depends not only on the particles, but also on the S-matrix.

By imposing periodic or anti-periodic boundary conditions for the wave function of bosons or fermions, respectively, one gets the following quantization rule for the momenta:

$$\exp(ip_i L) \prod_{j \neq i} S(\theta_i - \theta_j) = \pm 1 \tag{4.14}$$

or equivalently

$$m_i L \sinh \theta_i + \sum_{j \neq i} \sigma_{ij}(\theta_i - \theta_j) = 2\pi n_i \,, \tag{4.15}$$

where the numbers i runs from 1 to $\mathcal{N}$ and n_i is integer for bosons and semi-integer for fermions.

While solving the system Eq. (4.14) is hopeless, it turns out that its thermodynamic limit can be indeed managed. In the thermodynamic limit, both L and all $\mathcal{N}_a$ go to infinity in such a way that the densities $\mathcal{N}_a/L$ remain finite. The density of particles of species A_a with rapidity between θ and $\theta + \Delta\theta$ is indicated by $\rho_a^{(r)}(\theta)$. The energy density[2] can hence be written

$$E_L[\rho_a] = \sum_a \int_{-\infty}^{\infty} d\theta \rho_a^{(r)}(\theta) m_a \cosh \theta \,, \tag{4.16}$$

while the Bethe Ansatz equations Eq. (4.15) become

$$m_a \sinh \theta_i^{(a)} + \sum_b (\sigma_{ab} * \rho_b^{(r)})(\theta) = \frac{2\pi n_i^{(a)}}{L} \,, \tag{4.17}$$

where the convolution is defined in the usual way

$$(f * g)(\theta) = \int_{-\infty}^{\infty} \frac{d\tilde{\theta}}{2\pi} f(\theta - \tilde{\theta}) g(\tilde{\theta}) \,. \tag{4.18}$$

The integer numbers $n_i^{(a)}$ in Eq. 4.16 identify all the physically accessible levels: some of them, described by the density $\rho_a^{(r)}$, are actually occupied

[2]This energy density is denoted by E_L in order to distinguish it from the energy E_R defined in the previous section. On the cylinder they correspond to identifying the space with the non-compact or the compact dimensions, respectively.

(the corresponding rapidities $\theta_i^{(a)}$ are called *roots* of species a), other are free (*holes*), and their density is denoted by $\rho_a^{(h)}$. Obviously,

$$\rho_a(\theta) = \rho_a^{(r)} + \rho_a^{(h)} \,. \tag{4.19}$$

By differentiating Eq. (4.17) with respect to θ, we get

$$\rho_a(\theta) = \frac{m_a}{2\pi}\cosh\theta + \sum_b (\sigma'_{ab}(\theta) * \rho_b^{(r)})(\theta)\,, \tag{4.20}$$

where the prime denotes derivation with respect to θ. Remember that $\sigma(\theta)$ is proportional to the logarithm of the S-matrix (Eq. (4.13)), hence its explicit expression can be worked out for an integrable theory.

In the thermodynamic limit, to every pair of densities $\rho_a^{(r)}(\theta)$ and $\rho_a(\theta)$ correspond a large number of states, whose exact expression depends on the statistics of the particles:

$$\Omega_a = \frac{[\rho_a(\theta) L\Delta\theta]!}{[\rho_a^{(r)}(\theta)L\Delta\theta]![\rho_a^{(h)}(\theta)L\Delta\theta]!} \tag{4.21}$$

in the 'fermionic' case, and

$$\Omega_a = \frac{[\rho_a(\theta)L\Delta\theta + \rho_a^{(r)}(\theta)L\Delta\theta - 1]!}{[\rho_a(\theta)L\Delta\theta - 1]![\rho_a^{(r)}(\theta)L\Delta\theta]!} \tag{4.22}$$

in the 'bosonic' one. From these expressions one can estimate the entropy per unit length

$$\mathcal{S} = \ln(\prod_a \Omega_a)\,, \tag{4.23}$$

and therefore the free energy

$$Lf[\rho,\rho^{(r)}] = E_L[\rho^{(r)}] - \frac{1}{R}\mathcal{S}[\rho,\rho^{(r)}]\,. \tag{4.24}$$

To solve the thermodynamics means to minimize the free energy with respect to ρ and $\rho^{(r)}$, with the constraint Eq. (4.20). Note that, since we are interpreting the compact dimension as time, the inverse radius of the cylinder plays the role of the temperature. The explicit form of the entropy is

$$\mathcal{S}[\rho,\rho^{(r)}] = \sum_a \int_{-\infty}^{\infty} d\theta\, [\rho_a \ln\rho_a - \rho_a^{(r)}\ln\rho_a^{(r)} - (\rho_a - \rho_a^{(r)})\ln(\rho_a - \rho_a^{(r)})] \tag{4.25}$$

in the 'fermionic' case and

$$\mathcal{S}[\rho,\rho^{(r)}] = \sum_a \int_{-\infty}^{\infty} d\theta\, [(\rho_a + \rho_a^{(r)})\ln(\rho_a + \rho_a^{(r)}) - \rho_a\ln\rho_a - \rho_a^{(r)}\ln\rho_a^{(r)}] \tag{4.26}$$

in the 'bosonic' one. By using these expression in Eq. (4.24), we can minimize the free energy obtaining

$$m_a R\cosh(\theta) = \ln\frac{\rho_a - \rho_a^{(r)}}{\rho_a^{(r)}} + \sum_b \left(\sigma'_{ab} * \ln\frac{\rho_b}{\rho_b - \rho_b^{(r)}}\right)(\theta)\,. \tag{4.27}$$

This equation is usually written in terms of the pseudo-energies $\varepsilon_a(\theta)$ defined by

$$\exp(\varepsilon_a(\theta)) \pm 1 = \frac{\rho_a(\theta)}{\rho_a^{(r)}(\theta)}\,, \tag{4.28}$$

and of the dimensionless quantities

$$L_a(\theta) = \pm\ln[1 \pm \exp(-\varepsilon_a(\theta))]\,, \tag{4.29}$$

where the upper signum is for 'fermionic' case and the lower for 'bosonic' one. The final form of the TBA equations is

$$\hat{m}_a R\cosh\theta = \varepsilon_a(\theta) + \sum_b (\sigma'_{ab} * L_b)(\theta)\,, \tag{4.30}$$

where $\hat{m}_a = m_a/m_1$.

I spent some pages in the details of the derivation of the TBA equations because they give a way to exactly evaluate the bulk free energy:

$$f(R) = -\frac{1}{2\pi R}\sum_a \hat{m}_a \int_{-\infty}^{\infty} L_a(\theta)\cosh\theta d\theta\,. \tag{4.31}$$

Chapter 5

Truncation of conformal space

The truncation of conformal space approach has been invented by Yurov and Alexei Zamolodchikov [53]. It is an approximate method that gives numerical access to the spectrum of two-dimensional off-critical theories arising from deformation of minimal models as in Eq. (2.31). Unlike the methods reviewed in Sec. 2.3, however, the TCS works equally well for integrable and non-integrable deformations.

5.1 Conformal field theory on a cylinder

Let u, v be Cartesian coordinates on the cylinder: $-\infty < u < +\infty$, while $0 \leq v < R$. We can save notation by grouping them into the complex coordinate $w = u + iv$. The cylinder can now be conformally mapped onto the plane by means of the transformation

$$w \to z = R \exp\left(\frac{2\pi}{R} z\right) , \tag{5.1}$$

that is a shorthand for

$$(u, v) \to (x, y) = \left(R \cos v \exp\left(\frac{2\pi}{R} u\right), R \sin v \exp\left(\frac{2\pi}{R} u\right)\right) , \tag{5.2}$$

where $z = x + iy$. On the z-plane – indeed, on the Riemann sphere – the time evolution is radial, with $z = 0$ representing the far past and the point at infinity standing for the far future. This particular choice of the time direction leads to the so-called radial quantization of 2-D conformal field theory.

The holomorphic component $T(w) = -2\pi T_{ww}$ of the energy-momentum tensor under conformal transformations is changed according to the law [21]

$$T(w) \to T'(z) = \left(\frac{dz}{dw}\right)^{-2} T(w) + \frac{c}{12}\{w; z\}\,, \tag{5.3}$$

where the Schwarzian derivative is defined by

$$\{w; z\} = \frac{(d^3w/dz^3)}{(dw/dz)} - \frac{3}{2}\left(\frac{(d^2w/dz^2)}{(dw/dz)}\right)^2 . \tag{5.4}$$

The energy momentum tensor on the cylinder and that on the plane are thus related by the condition:

$$T_{\text{cyl.}}(w) = \left(\frac{2\pi}{R}\right)^2 \left\{z^2 T_{\text{pl.}}(z) - \frac{c}{24}\right\} . \tag{5.5}$$

The vacuum energy density of a conformal theory vanishes on the plane, $\langle z^2 T_{\text{pl.}}(z)\rangle = 0$, as a result of the expansion (2.10) and of the vacuum definition (2.22). It should be so, as the conformal theory is massless and doesn't possess any natural scale. On the cylinder, however, the compactification radius provides an obvious (inverse) mass unit, and the vacuum expectation value of the energy momentum tensor is non-zero:

$$\langle T_{\text{cyl.}}(w)\rangle = -c\frac{\pi^2}{6R^2} . \tag{5.6}$$

The central charge is therefore interpreted as a Casimir energy [54, 55]: the shift in the vacuum energy density caused by the finite size of the cylinder.

Actually, the last equation is correct only for unitary minimal models: the vacuum as defined in Eq. (2.22) is not the lowest energy state if the theory contains operators with negative conformal dimensions. Indeed, for any highest-weight vector $|h\rangle$ defined in Eqs. (2.12) and (2.13), we have

$$\langle h|z^2 T(z)|h\rangle = \langle h|\sum_{n\in\mathbb{Z}} z^{-n} L_n|h\rangle = h\,. \tag{5.7}$$

In writing the first equality we used the mode expansion (2.10), while the second equality assumes $\langle h|h\rangle = 1$. The expectation value $\langle z^2 T(z)\rangle \equiv \langle 0|z^2 T(z)|0\rangle$ must be fixed equal to h_{min}, that is the lowest conformal weight of the Kac table (0 if the theory is unitary, negative otherwise). The central charge must therefore be replaced by the effective central charge $\tilde{c} = c - 24h_{\text{min}}$. For any minimal model the central charge is positive and lesser than 1.

In the framework of radial quantization, the time translation on the plane is just a scale transformation, so its generator is $-z\partial_z - \bar{z}\partial_{\bar{z}}$, that corresponds to $L_0 + \bar{L}_0$. The transfer matrix on the torus Eq. (4.8) is therefore written

$$\mathcal{T} = \exp\left(-\frac{2\pi a}{R}(L_0 + \bar{L}_0 - c/12)\right), \tag{5.8}$$

so that the partition function Eq. (4.6) reads

$$Z = \mathrm{Tr}\,\mathcal{T}^M = \mathrm{Tr}\exp\left(-2\pi\frac{L}{R}(L_0 + \bar{L}_0 - c/12)\right). \tag{5.9}$$

In the last two formulas, the Hamiltonian is normalized in such a way that the free energy per unit area vanishes in the bulk.

Let us now consider the R-dependence of the free energy. We have to scale the compact dimension $R \to R(1+\epsilon)$ and see the effect of such a rescaling on the free energy, by means of the definition Eq. (A.6) of the energy-momentum tensor:

$$\delta\mathcal{W} = -\frac{1}{2}\int du\, dv\, \sqrt{|g|}\delta g_{\mu\nu}\langle T^{\mu\nu}\rangle\,. \tag{5.10}$$

The variation of the radius is realized by means of the coordinate transformation

$$w - \bar{w} \to w' - \bar{w}' = (1+\epsilon)(w - \bar{w}) \tag{5.11}$$

$$w + \bar{w} \to w' + \bar{w}' = w + \bar{w}\,. \tag{5.12}$$

Note that this is not a conformal transformation. The variation of the metric is

$$\delta g_{\mu\nu} = \frac{\epsilon}{2}\begin{pmatrix} 1 & -1 \\ -1 & 1 \end{pmatrix}, \tag{5.13}$$

hence about the connected functional we find

$$\begin{aligned} \delta\mathcal{W} &= -\frac{1}{2}\int dw\, d\bar{w}\, \sqrt{|g|}\frac{\epsilon}{2}\left(\langle T^{ww}\rangle + \langle T^{\bar{w}\bar{w}}\rangle\right) \\ &= -\int dw\, d\bar{w}\, \sqrt{|g|}\frac{\delta R}{R}\frac{\pi\tilde{c}}{6R^2}\,. \end{aligned} \tag{5.14}$$

In order to perform the integration it is convenient to convert to real variables u, v: the integration in v gives a factor R, while the integral in u is exploited to define a free energy per unit length of the cylinder $f = \lim_{L\to\infty}\mathcal{W}/L$:

$$\delta f = \frac{\pi\tilde{c}}{6R^2}\delta R\,, \tag{5.15}$$

that after integration yields

$$f(R) = -\frac{\pi\tilde{c}}{6R}\,. \tag{5.16}$$

5.2 Off-critical theory on a cylinder

We have yet analyzed what happens to the conformal theory when put on a cylinder. Now we study the effect of deforming the CFT by means of one of its relevant scalar operators φ_i. If we assume that the coupling is small, we can adopt a perturbative viewpoint and let the modified Hamiltonian act on the unperturbed (conformal) Hilbert space. The perturbed Hamiltonian is

$$\hat{H}_i = \hat{H}_0 + \hat{V}_i\,, \tag{5.17}$$

where $\hat{H}_0$ is the conformal Hamiltonian on the cylinder

$$\hat{H}_0 = \frac{2\pi}{R}\left(L_0 + \bar{L}_0 - \frac{c}{12}\right)\,, \tag{5.18}$$

and the interaction is formally defined by

$$\hat{V}_i = g_i \int_0^R dv \left(\frac{2\pi}{R}\right)^{2h_i} \varphi_i(u,v)\,. \tag{5.19}$$

Since we choose φ_i to be scalar, the momentum operator on the cylinder

$$\hat{K} = \frac{2\pi}{R}(L_0 - \bar{L}_0) \tag{5.20}$$

is preserved by the Hamiltonian evolution.

The matrix elements of $\hat{V}_i$ between conformal states can be reduced to the evaluation of three-point functions on the plane:

$$\langle\varphi_j|V_i|\varphi_k\rangle = \frac{R}{2\pi}\langle\varphi_j|\varphi_i(0,0)|\varphi_k\rangle\delta_{K_i,K_j}\,. \tag{5.21}$$

As we have already seen in Sec. (2.2.1), the Hilbert space is organized in Verma modules. Once the matrix elements of V_i between primary states are known, any other element is evaluated by means of the relations

$$[L_n - L_0, \varphi_j(0)] = nh\varphi_j(0) \tag{5.22}$$

$$[\bar{L}_n - \bar{L}_0, \varphi_j(0)] = n\bar{h}\varphi_j(0)\,. \tag{5.23}$$

The matrix elements between primary fields are just the structure constants of the operator algebra

$$\langle\varphi_j|\varphi_i(0)|\varphi_k\rangle = \left(\frac{2\pi}{R}\right)^{2h} C_{\varphi_j,\varphi_i,\varphi_k}\,. \tag{5.24}$$

These structure constants for minimal models are calculated in general form in Ref. [36, 37]. Table 3.3 gives the structure constants for the tricritical Ising model.

5.3 Truncated Hamiltonian

The Hamiltonian acting on the Hilbert space is of course infinite dimensional; we need to truncate the conformal space if we want to be able to compute anything. In my thesis the truncation is performed by discarding the states of level 6 or more in each Verma module. For the tricritical Ising model, this amounts to keep 228 states. The suitable truncated basis of the Hilbert space and the matrix elements of $\hat{H}_0$ and $\hat{V}_i$ have been computed by means of a program for Mathematica written by Lässig and Mussardo [56]. The numerical diagonalization of the Hamiltonians was performed by the NAG routines of Maple.

This is a good place to say something about the precision of this approach. There is no theoretical control over the error introduced by the truncation. In Ref. [3], the ground state energy for fixed R was evaluated at different truncation levels l and then axtrapolated to $l \to \infty$ by fitting the formula

$$E_0^{(l)}(R) = s_0(R) + s_1(R) l^{-s_2(R)} . \tag{5.25}$$

Although this procedure worked well in their case, it must be remarked that this formula lacks theoretical justification. However, the high precision of Fonseca and Zamolodchikov's numerical estimates is due above all to the fact that, dealing with the Ising model, they can exploit the free fermion basis, so that one of the two conformal perturbations is treated exactly (see Eq. (1.17)). This lucky accident is a peculiarity of the Ising model. Since I could not have reached such high precision anyway, I rather focused on the objective of gaining a qualitative understanding of the analytic structure of the free energy.

A typical spectrum obtained by TCS is given in Fig. (5.1). The first 12 levels of the theory $\mathcal{A}_2^+$ (defined in Sec. 3.2) are plotted against $r = R|g_2|^{9/5}/(2\pi)$. The lowest lines correspond to the ground state E_0 and the four lowest masses. Note how above the threshold $E = 2m_1$ we can find level crossings, signal of the integrability of the theory. In order to give an idea of the errors associated to this method, we can compare the exact masses of Tab. 3.8 with the energy differences $\Delta E_i = E_i - E_0$, as in Fig. 5.2. It is quite evident that the TCS works better for the lowest masses. Another feature of TCS well exemplified by Fig. 5.2 is the existence of a physical window: we are interested in infrared data, that is in the limit $r \to \infty$, but as r increases, the truncation effects become more and more relevant.

The best precision, of course, is achieved when studying the ground state. In this case, the standard method to choose the physical window is to look

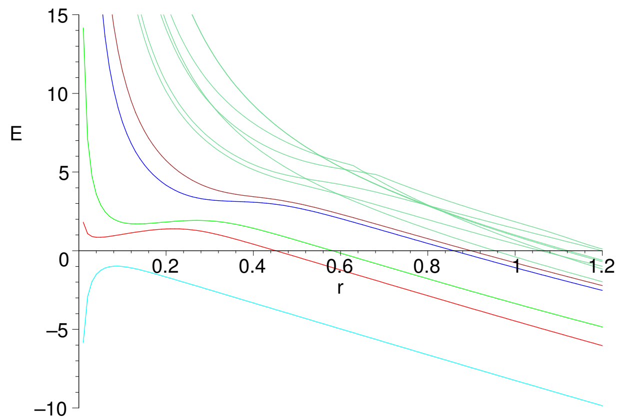

Figure 5.1: Spectrum of the theory $\mathcal{A}_2^+$: the first 12 levels.

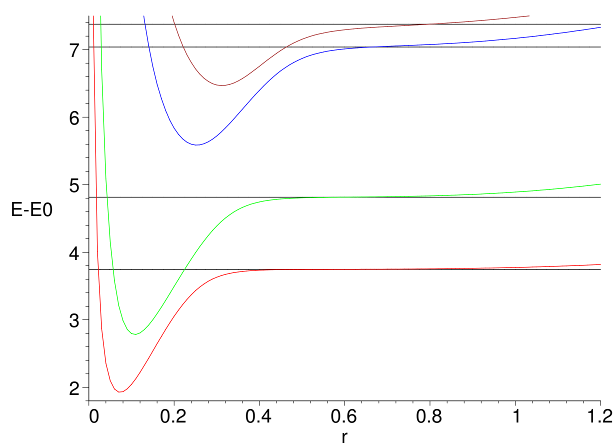

Figure 5.2: Spectrum of the theory $\mathcal{A}_2^+$: the black lines are the exact masses, the colored ones are energy levels differences $\Delta E_i = E_i - E_0$ as computed by TCS.

at the effective scaling exponent of the ground state energy:

$$\alpha = \frac{R}{E}\frac{dE}{dR}. \tag{5.26}$$

The physical window is characterized by $\alpha \approx 1$. For excited levels, α is not a good indicator because it diverges when $E = 0$. I found it convenient to look at the effective scaling exponent of the differences:

$$\alpha' = \frac{R}{E - E_0}\frac{dE}{dR}, \tag{5.27}$$

selecting the physical window in the region where $\alpha' \approx 0$.

Chapter 6

Free energy of TIM

This chapter collects the results of my research about the free energy of the tricritical Ising model. After introducing my notations in the first section, I discuss the analytic structure of the theory simultaneously deformed by the leading magnetic and thermic perturbations (the case more similar to the Ising field theory) in Secs. 6.2 and 6.3. The effect of turning on the sub-leading energy perturbation is treated in Sec. 6.4. Some interesting byproducts of my numerical data are collected in the last section.

6.1 Conventions

In this thesis I am concerned with the quantum field theory formally defined on a cylinder of circumference R by the action

$$\mathcal{A}[g_1, g_2, g_3, g_4] = \mathcal{A}_{(c=7/10)} + \sum_{i=1}^{4} g_i \int_{-\infty}^{\infty} du \int_0^R dv \, \varphi_i(u, v) \,, \tag{6.1}$$

where the fields $\varphi_i(u, v)$ are defined in Tab. 3.2. I will outline location and nature of the singularities of the free energy by considering two- or three-dimensional slices of the total four-dimensional parameter space. When considering such a slice, I will write explicitly only those couplings that are different by 0: for instance,

$$\mathcal{A}[g_1, g_2, 0, 0] \equiv \mathcal{A}[g_1, g_2] \,. \tag{6.2}$$

Sometimes it is important to stress that, say, g_2 is negative or g_1 is imaginary. In such occasions, $|g_i|$ is denoted by the appropriate one among the following symbols:

$$h \equiv |g_1| \qquad \tau \equiv |g_2| \qquad h' \equiv |g_3| \qquad \chi \equiv |g_4| \,. \tag{6.3}$$

To give an example, $\mathcal{A}[-\tau, ih']$ means $\mathcal{A}[g_2, g_3]$ with g_2 real and negative, g_3 purely imaginary with positive imaginary part.

The same convention applies to the correspondent Hamiltonian:

$$\hat{H}[g_1, g_2, g_3, g_4] = \hat{H}_0 + \sum_{i=1}^{4} g_i \int_0^R dv\, \hat{\varphi}_i(u, v)\,, \tag{6.4}$$

where the hat indicates quantities defined on the cylinder:

$$\hat{H}_0 = \frac{2\pi}{R}\left(L_0 + \bar{L}_0 - \frac{c}{12}\right) \tag{6.5}$$

$$\hat{\varphi}_i = \left|\frac{2\pi}{R}\right|^{2h_i} \varphi_i\,. \tag{6.6}$$

Several dimensionless ratios between the coupling constants are used in this chapter: I think it is useful to collect all the definitions here for a quick reference:

$$\xi = \frac{g_1}{|g_2|^{77/72}} \qquad \eta' = \frac{g_2}{|g_1|^{72/77}} \tag{6.7}$$

$$\zeta' = \frac{g_4}{|g_1|^{32/77}} \qquad \eta = \frac{g_2}{g_1^{72/77}} \tag{6.8}$$

Throughout this chapter, I assume $g_2, g_4 \in \mathbb{R}$: it is sensible to study the analytic properties of the free energy in complex temperature [57, 58] or chemical potential, but I don't want to enter this problem now. The magnetic field g_1 is assumed to be real in the next section, and complex in Sec. 6.3. It would have been equally interesting to study the analyticity in the subleading magnetic field g_3, but since $h_3 = 7/16$, the ultraviolet divergences quickly spoils the TCS of any attendibility, at least as far as the evaluation of the ground state is concerned.

6.2 Free energy of $\mathcal{A}[g_1, g_2]$: real couplings

We will in this section begin the systematic exploration of the analytic properties of the free energy. The Hamiltonian $H[g_1, g_2]$ appears to be the best starting point for at least two reasons: first, the TCS produces the most accurate results when the most relevant perturbations are present; moreover, the affinity with the Ising field theory can provide a valuable source of inspiration. Let us then consider the doubly deformed Hamiltonian

$$H[g_1, g_2] = \frac{2\pi}{R}\left[H_0 + 2\pi g_1 \left(\frac{R}{2\pi}\right)^{77/40} V_1 + 2\pi g_2 \left(\frac{R}{2\pi}\right)^{9/5} V_2\right]. \tag{6.9}$$

We assume $g_2 \neq 0$ and fix $|g_2|^{5/9}$ as the mass unit of measure. Then we introduce dimensionless Hamiltonian $\mathcal{H}_\pm = H/|g_2|^{5/9}$ and cylinder radius $r = R|g_2|^{5/9}/(2\pi)$, so that we can write

$$\mathcal{H}_\pm(\xi) = \frac{1}{r}\left[H_0 + 2\pi\xi r^{77/40}V_1 \pm 2\pi r^{9/5}V_2\right] \tag{6.10}$$

where the signum is plus in the high-temperature regime $g_2 > 0$ and minus in the low-temperature one $g_2 < 0$, while ξ is defined by Eq. (6.7), with g_1 real.

The free energy density, that can be extracted from the behavior of the ground state of the Hamiltonian (6.9) by means of the relation (4.10), having dimensionality of a squared mass, can be written

$$F(g_1, g_2) = |g_2|^{10/9}(\mathcal{E}_0 + \mathcal{F}(\xi))\,, \tag{6.11}$$

where $\mathcal{E}_0$ is exactly known [43]

$$\begin{aligned} \mathcal{E}_0 &= -\frac{\sin(2\pi/9)}{8\sin(\pi/3)\sin(5\pi/9)}\mathcal{C}_2^2 = -1.32155588\ldots \\ \mathcal{C}_2 &= \frac{2\Gamma(2/9)}{\Gamma(2/3)\Gamma(5/9)}\left(4\pi^2\frac{\Gamma(2/5)}{\Gamma(3/5)}\left(\frac{\Gamma(4/5)}{\Gamma(1/5)}\right)^3\right)^{5/18}, \end{aligned} \tag{6.12}$$

and $\mathcal{F}(\xi)$ is the dimensionless free energy density.

For practical and conceptual reasons, it is convenient to split the space of couplings into high- and low-temperature sectors and treat them separately. In the region $g_2 > 0$, indeed, the keywords are distribution of zeros of partition function and Yang–Lee (in fact, Yang–Lee-like) edge singularity, while for $g_2 < 0$ the relevant physical ideas are metastable vacuum decay and spinoidal singularity. These two regimes, however, are deeply related, and we will show how one can make full use of this relationship.

In the high-temperature regime, $\mathcal{F}_{\text{high}}(\xi)$ is even: $\mathcal{F}_{\text{high}}(\xi) = \mathcal{F}_{\text{high}}(-\xi)$, as a consequence of the $\mathbb{Z}_2$ spin-reversal symmetry. No phase transition is present for $g_2 > 0$, hence we can expand $\mathcal{F}$ around $\xi = 0$ writing the convergent series

$$\mathcal{F}_{\text{high}}(\xi) = \mathcal{F}_2\xi^2 + \mathcal{F}_4\xi^4 + \mathcal{F}_6\xi^6 + \ldots\,. \tag{6.13}$$

The coefficient $\mathcal{F}_2$ is proportional to the high-temperature susceptibility at $h = 0$ that can be estimated either by integrating the two-spin correlation function

$$\int d^2x < \varphi_1(x)\varphi_1(0) >_c\,, \tag{6.14}$$

or by using the TCS. My best estimate, obtained by fitting the TCS spectra for different values of ξ, is

$$\mathcal{F}_2 = -\frac{\Gamma_{11}^{2+}}{2} = -0.046(9)\,, \tag{6.15}$$

where the notation Γ_{11}^{2+} for the susceptibility is borrowed from Ref. [40]. As far as I know, no data about higher order coefficients is available at the moment. In principle, one could use form factor expansion of the four-spin correlation function in order to determine $\mathcal{F}_4$, like the authors of Ref. [59] did for the Ising model, but no attempt has been done of computing three-particle form factors for the tricritical Ising[1] model.

In the low-temperature regime, if one tries to smoothly vary the magnetic field from a positive value to a negative one, at $\xi = 0$ one has residual magnetization which does not disappear immediately as ξ becomes negative. The system enters a metastable phase in $\xi = 0$, where a weak singularity is predicted by Langer theory. The spin-reversal symmetry being spontaneously broken, the function $\mathcal{F}_{\text{low}}(\xi)$ is not even: its asymptotic expansion reads

$$\mathcal{F}_{\text{low}}(\xi) = \widetilde{\mathcal{F}}_1\xi + \widetilde{\mathcal{F}}_2\xi^2 + \widetilde{\mathcal{F}}_3\xi^3 + \dots\,. \tag{6.16}$$

The first coefficient $\widetilde{\mathcal{F}}_1$ is the spontaneous magnetization at $g_1 = 0$: it can be exactly evaluated [60]

$$\widetilde{\mathcal{F}}_1 = -B_{12} = -1.59427\dots\,. \tag{6.17}$$

Again, the conventions of Ref. [40] are assumed. The second coefficient $\widetilde{\mathcal{F}}_2$ is related to the low-temperature susceptibility Γ_{11}^{2-}. My estimate (see Tab. 6.1 for a comparison with results obtained by means of other approaches) is

$$\widetilde{\mathcal{F}}_2 = -\frac{\Gamma_{11}^{2-}}{2} = -0.011(8)\,. \tag{6.18}$$

No other term is available at the moment. Also in this case, the determination of further coefficients requires the computation of multi-spin correlation functions.

[1]The main obstacle is that the error associated to the one- and two-particle form factors propagate while solving the system of linear equations needed to build the three-particle ones. While for the Ising case one can determine the lowest form factors with the desired precision, this is not possible for TIM [40].

6.3 Free energy of $\mathcal{A}[g_1, g_2]$: complex magnetic field

In this section we analytically continue the magnetic field g_1 (and therefore ξ) to complex values. The Hamiltonian to be diagonalized is still given by Eq. (6.10), but its eigenvalues are in general complex numbers. For the Yang–Lee theorem, we expect the free energy $\mathcal{F}(\xi)$ to be analytic in some neighborhood of $\xi = 0$ in the high-temperature plane; in the low-temperature plane, if the analytic continuation starts from the positive real axis, we expect analyticity at least in the right half-plane. It is useful to keep in mind, for a comparison, the results of Fonseca–Zamolodchikov's analysis of the Ising model, summarized in Figs. (1.3) and (1.5).

6.3.1 High-temperature regime

The first problem to solve is to determine the convergence radius of the expansion Eq. (6.13), that amounts to locate the essential singularities created by the accumulation of zeros of the partition function. The distribution of Yang–Lee zeros in the Blume–Capel model has been studied for the first time by Suzuki [61] (see also [62, 63]). He proved that all the poles of the free energy are located on the imaginary axis of the complex H-plane, just like in the Ising model, provided that $\beta\Delta < \ln 2$, that is, loosely speaking, if the dilute Ising model is not too dilute. For $\beta\Delta > \ln 2$, the zeros lie on arcs that can possibly have no intersection at all with the imaginary axis [64, 65]. In the mean-field approximation, the tricritical point Eq. (1.7) is characterized by $\beta_t\Delta_t = 2\ln 2$, hence should be out of the region where Suzuki's result is valid. However, the mean-field approximation should not be taken too seriously in two dimensions, so we have better to guess the position of the singularities of the free energy by carefully inspecting the TCS results without prejudices.

If we look back at the Hamiltonian (6.9), we easily realize that ξ is not the only dimensionless ratio between couplings we can define. Indeed, we can decide to measure the masses in units of $|g_1|^{40/77}$, so that instead of Eq. (6.10) we get

$$\mathcal{H}'_{\arg(g_1)}(\eta') = \frac{1}{r'}\left[H_0 + 2\pi e^{i\arg(g_1)} r'^{77/40} V_1 + 2\pi\eta' r'^{9/5} V_2\right], \tag{6.19}$$

where

$$\eta' = \frac{g_2}{|g_1|^{72/77}}. \tag{6.20}$$

Note that with this definition η' is always real, even for complex g_1. Moreover, in this variable the high- and low-temperature regimes are analyzed together. The spectrum obtained by diagonalizing the Hamiltonian (6.19) is obviously related to the one extracted from Eq. (6.10) by means of the relations

$$E' = E\eta'^{5/9} \qquad\qquad r = r'\eta'^{5/9}\,. \tag{6.21}$$

The spectrum of the Hamiltonian $H[g_1, g_2]$ can thus be studied in terms of ξ in the region where $|g_1|$ is small, while η' provides access to the spectrum for large values of $|g_1|$: by combining the two approaches one can be confident of not missing relevant phenomena.

Inspired by the Ising case, I looked for the presence of singularities on the imaginary axis of the ξ plane ($\arg(g_1) = \pi/2$). Figure 6.1 shows the real part of the three lowest levels of the spectrum of $\mathcal{H}'_{\pi/2}$ for different values of η'. Few explanations are in order here. The analytic continuation of ξ to complex values does not spoil the spin-reversal symmetry, hence the spectrum is still invariant for the transformation $\xi \to -\xi$. When ξ is purely imaginary, we have $-\xi = \xi^*$ so the $\mathbb{Z}_2$ symmetry becomes invariance of the spectrum under complex conjugation. Therefore the eigenvalues of $\mathcal{H}'_{\pi/2}$ must be real, or come in complex conjugate pairs. It is easy to distinguish the region $\eta' > \eta'_c$, where (for values of R within the physical window) the ground state is real while the second and third levels form a complex conjugate pair, from the region $\eta' < \eta'_c$, where the ground state is complex and the third level is real. The critical value is $0.0419 < \eta'_c < 0.0420$. One can check that $\mathcal{H}_+(\xi)$ shows the same transition for

$$29.67i < \xi_c < 29.74i\,. \tag{6.22}$$

Since a careful inspection gives no other singular point (except, of course, the complex conjugate of ξ_c), we can cut the high-temperature ξ plane just in the same fashion of the Ising model (see Fig. 6.3(b)).

Which non-unitary minimal model is related to the edge singularity that arises in TIM? To my knowledge, the only published paper about this interesting question was authored by von Gehlen [66], who applied finite-size-scaling methods to a quantum chain which can be defined starting from a strongly anisotropic Blume–Emery–Griffiths model [67]. At the end of his analysis, von Gehlen claimed that his data "strongly hint" that the relevant conformal field theory is the minimal model $\mathcal{M}(7,2)$. In principle, TCS gives direct access to the effective central charge through the relation, valid at the critical point,

$$E_0(R) = F_0 R - \frac{\pi\tilde{c}}{6R} + \mathcal{O}\left(\frac{1}{R^2}\right) \tag{6.23}$$

(more terms can be found in Ref. [3]). In point of fact, a great precision is needed in order to properly evaluate the subleading behavior of the ground state energy. At level 5 of truncation, it is not even possible to discriminate between $\tilde{c} = 17/20$ as in $\mathcal{M}(8,5)$ and the value $\tilde{c} = 4/7$ characteristic of $\mathcal{M}(7,2)$, let alone the small difference separating the latter and $\tilde{c} = 3/5$ related to the third candidate $\mathcal{M}(5,3)$. As the direct way fails, one can try to generalize the arguments leading to the identification of the Yang–Lee edge singularity arising in the Ising model. This smart way too meet some interesting difficulties. A report of my (unsuccessful) attempt may be found in App. B.

6.3.2 Low-temperature regime

The functions $\mathcal{F}_{\text{high}}(\xi)$ and $\mathcal{F}_{\text{low}}(\xi)$ are obviously related one to another. We already introduced with Eq. (6.20) a variable which describes both the high- and low-temperature sectors. However, η' is a real variable: in order to connect the analytic structure of the high- and low-temperature ξ planes we need a variable which is analytically related to ξ. It is sufficient to change the definition of η' by removing the modulus in the denominator:

$$\eta = \frac{g_2}{g_1^{72/77}} \, . \tag{6.24}$$

Now we have a complex variable suitable for describing both the temperature regimes, and analytically related to ξ:

$$\eta = \pm \frac{1}{\xi^{72/77}} \, , \tag{6.25}$$

where the signum is '+' for the high-temperature sector and '-' for the low-temperature one.

The η plane is graphically represented in Fig. 6.3(c). The right half-plane of the high-temperature ξ-plane is mapped by Eq. (6.25) into the corner $-\frac{36}{77}\pi < \arg(\eta) < \frac{36}{77}\pi$, while the image of the right half-plane of the low-temperature ξ-plane is the region $-\frac{36}{77}\pi < \arg(-\eta) < \frac{36}{77}\pi$. The Yang–Lee-like branching points are mapped into the points $\eta = Y_c \exp(\pm i \frac{36}{77}\pi)$, where $Y_c = 1/|\xi_c|^{72/77}$. From the Fig. 6.3(c) it is evident what we can expect when, in the low-temperature ξ-plane, we move from the real positive axis: we have clear way (that is, the free energy can be safely analytically continued) until we reach the imaginary axis, where we meet a branch cut that is just what in the high-temperature ξ-plane appears as the Yang–Lee-like branch cut (see Fig. 6.2).

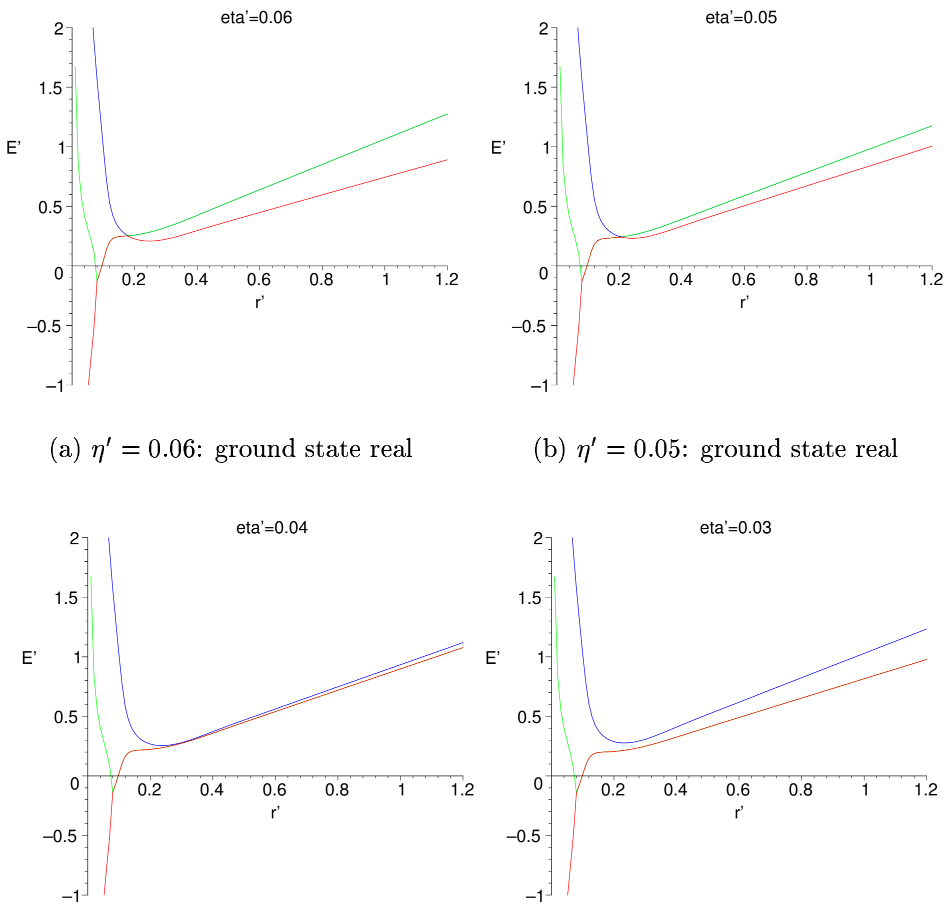

(a) $\eta' = 0.06$: ground state real

(b) $\eta' = 0.05$: ground state real

(c) $\eta' = 0.04$: ground state complex

(d) $\eta' = 0.03$: ground state complex

Figure 6.1: Spectrum of $\mathcal{H}'_{\pi/2}(\eta')$: real parts of the three lowest eigenvalues. When two lines overlap because they are forming a conjugate pair, only the color of the lowest one is showed. The critical value is $0.0419 < \eta'_c < 0.0420$.

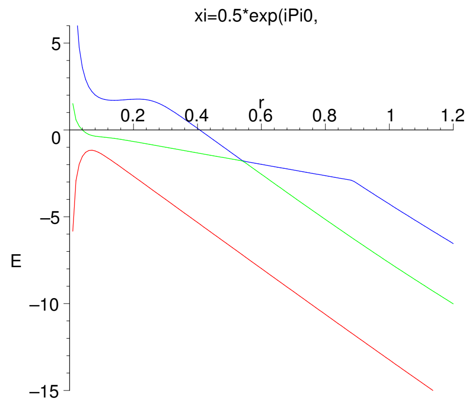

(a) $\xi = 0.5$

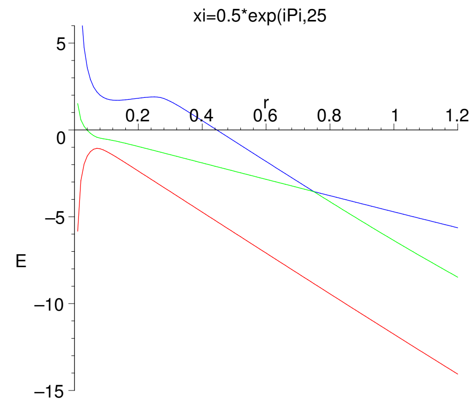

(b) $\xi = 0.5e^{i\pi/4}$

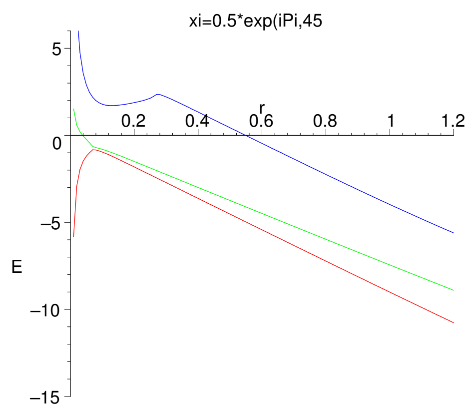

(c) $\xi = 0.5e^{i\pi 9/20}$

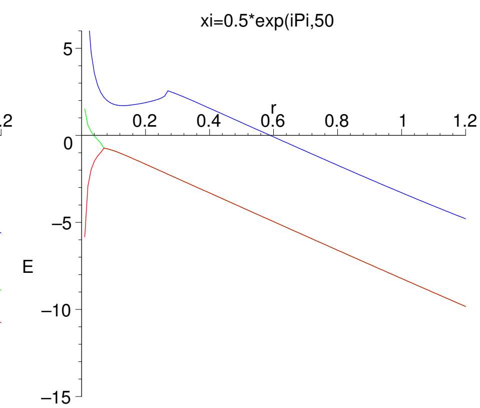

(d) $\xi = 0.5e^{i\pi/2}$

Figure 6.2: Spectrum of $\mathcal{H}_{-}(\xi)$: real parts of the three lowest eigenvalues. As ξ is rotated into the complex plane, the ground state and the false vacuum line get close, until they eventually form a complex conjugate pair when ξ reaches the imaginary axis.

Indeed, the spectra obtained by means of TCS show that the exponential splitting amongst the first two levels, that is the effect of the non-zero amplitude of tunnelling between the two degenerate vacua, is removed as soon as an imaginary magnetic field, however small, is turned on. So the ground state is complex for any imaginary ξ. The TCS permits also to determine the nature of the branch cut: it is sufficient to examine the imaginary part of the ground state to realize that the values of the free energy on opposite edges of the cut are complex conjugate. This is exactly the behavior we expect on the ground of the critical droplets calculations of the metastable vacuum decay [68, 69].

The position of the singularities has physical meaning, but cutting the plane is a matter of conventions; in particular, we can, following Fonseca and Zamolodchikov, draw a cut passing through zero in the high-temperature ξ plane, so that in the η plane we have cleared the way for going into the low temperature sector while remaining close to the real axis, where $\mathcal{F}(\eta)$ is analytic. On the low-temperature ξ plane, this operation removes the branch cut along the imaginary axis, and we can extend the analytic continuation into the left half-plane. Note however an interesting difference with respect to the Ising case: we cannot expect to be able to continue the free energy until we reach the negative real axis. Due to the larger angle of rotation (determined by the conformal dimensions of the operators involved), we meet the edge singularities at the points $\xi = |\xi_c| e^{\pm i\pi 41/72}$, where $|\xi_c| \approx 29.7$.

For the Ising free energy, one knows where the spinoidal point and the Yang-Lee edge singularities are: the extended analiticity conjecture fills the gap in between in the η plane (see Fig. 4 in Ref. [3]) so that we can state they are the same singularity. Here, we have no 'shadow domain' to make conjectures upon, the fact that the branching points we meet in the low-temperature left half-plane are precisely the edge singularities is granted, what we lack is an interpretation for these points in the context of the low-temperature physics. It is very appealing to identify them with a pair of complex conjugate spinoidal points: also the position, with that little negative real part, conjures in suggesting the picture of the tricritical counterpart of the spinoidal point on the real axis of the Ising model splitted in two after somehow being given an imaginary part.

6.4 Free energy of $\mathcal{A}[g_1, g_2, g_4]$

Once the analytic structure is revealed in the $g_3 = g_4 = 0$ plane, we can try to explore what happens if one turns on a small perturbation in the chemical potential. Due to the fact that $h_4 = 3/5$ is well above the critical value $1/2$

for the appearance of ultraviolet divergences, the TCS can probe only a small region around $g_4 = 0$. What emerges neatly is the fact that increasing g_4 the Lee–Yang-like branch points get closer to the real axis. Actually, this agrees with the overall picture I presented so far. Let us see why.

The theory $\mathcal{A}_4^+$ describes the massless flow between the tricritical and the usual Ising model. From lattice viewpoint, this is related to the fact that if in the Blume–Capel model we send $\Delta \to -\infty$, then the spin-0 mode is decoupled and we recover the Ising model. Along this renormalization group flow, the conformal dimension of the magnetic field changes from 3/80 to 1/16 while the conformal dimension of the thermal perturbation evolves from 1/10 to 1/2. Hence the dimensionless ratio $\xi = g_1/|g_2|^{77/72}$ is turned into its Ising counterpart $\xi_{\rm IM} = g_1/|g_2|^{15/8}$. This implies that the critical values of ξ identifying the position of the edge singularity are comparable, therefore I expect that along the flow generated by $g_4 > 0$ the value $|\xi_c| \approx 29.7$ is lowered up to $|\xi_c| \approx 0.0060335(7)$ that is the position of the edge singularity in the Ising model [3]. By the same token, I expect that as $g_4 \to -\infty$ the edge singularities are moved more and more far from the real axis, since if I remove the values ± 1, no phase transition is possible.

Of course, I cannot claim that the observed behavior, within a range $-0.01 < \zeta' < 0.01$ (ζ' is defined by Eq. (6.8)) is a proof of whatsoever: the best I can say is that it is a step in the expected direction.

6.5 Amplitudes and RG flows

An extensive study about the universal amplitude ratios for the tricritical Ising model in two dimensions has been recently performed by Fioravanti, Mussardo, and Simon [40]. In their paper, the truncation of conformal space is applied to the theories defined by the perturbed actions

$$\mathcal{A}_i = \mathcal{A}_{(c=7/10)} + g_i \int d^2x\, \varphi_i(x) \qquad i = 1, \ldots, 4\,. \tag{6.26}$$

Since they use the eigenvectors of the truncated Hamiltonian to determine the vacuum expectation values of the primary fields [70], the authors of Ref. [40] are able to evaluate the susceptibilities without introducing a second perturbation. In my study of the free energy, I computed some of these susceptibilities by means of the doubly perturbed Hamiltonians

$$\mathcal{A}_{ij} = \mathcal{A}_{(c=7/10)} + g_i \int d^2x\, \varphi_i(x) + g_j \int d^2x\, \varphi_j(x)\,, \tag{6.27}$$

thus obtaining as a byproduct an internal consistency check of the TCS approach. The amplitudes I computed are collected in table 6.1 together

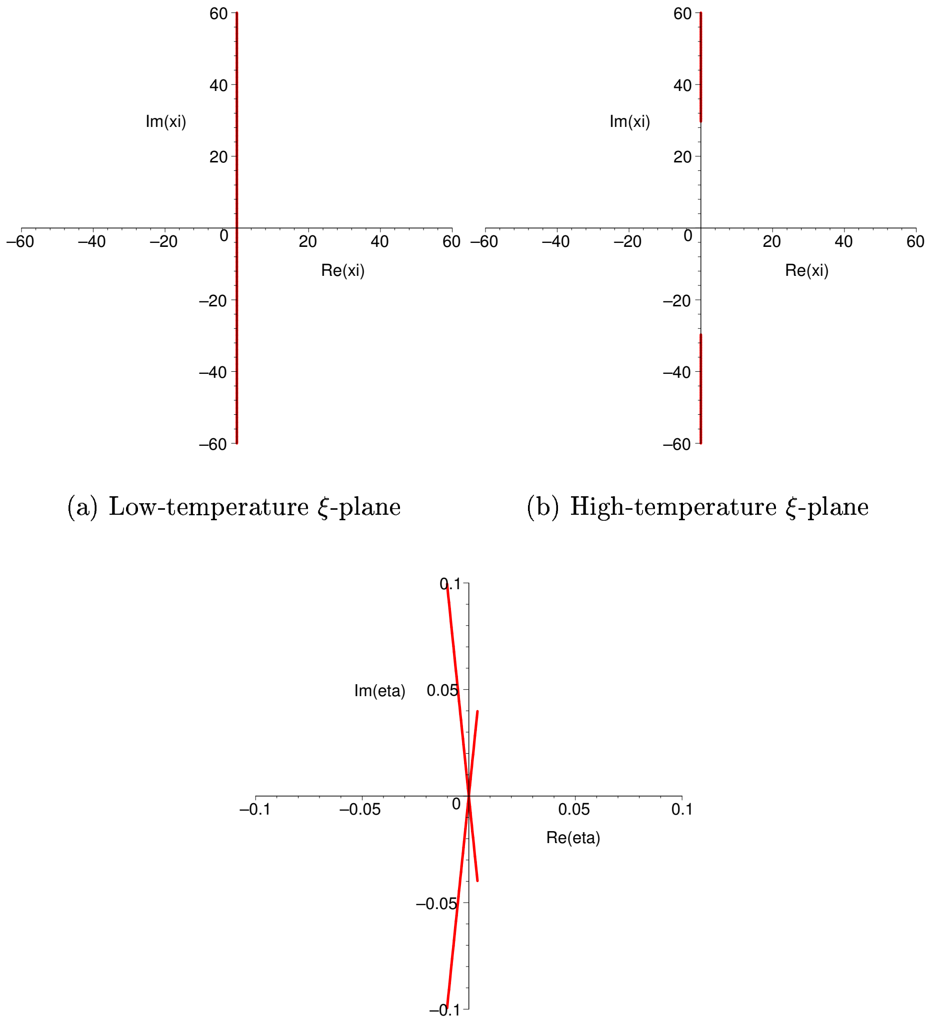

(a) Low-temperature ξ-plane

(b) High-temperature ξ-plane

(c) η-plane

Figure 6.3: The branch cuts of the theory $\mathcal{A}[g_1, g_2]$. The high-temperature right half-plane is mapped into the corner $-\frac{36}{77}\pi < \arg(\eta) < \frac{36}{77}\pi$, while the low-temperature right half-plane is mapped into the region $-\frac{36}{77}\pi < \arg(-\eta) < \frac{36}{77}\pi$.

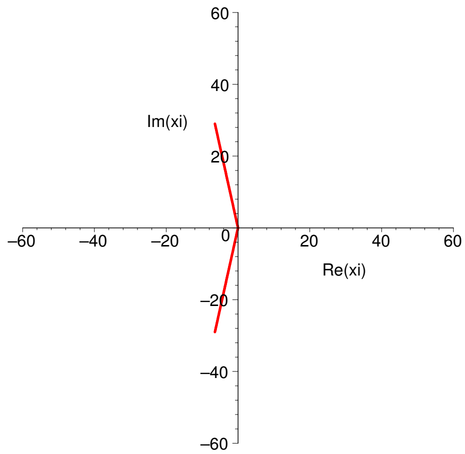

(a) Low-temperature ξ-plane

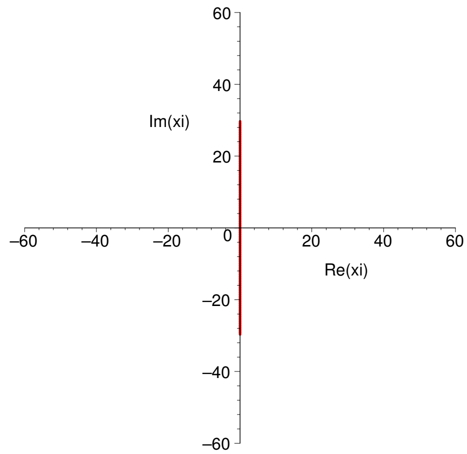

(b) High-temperature ξ-plane

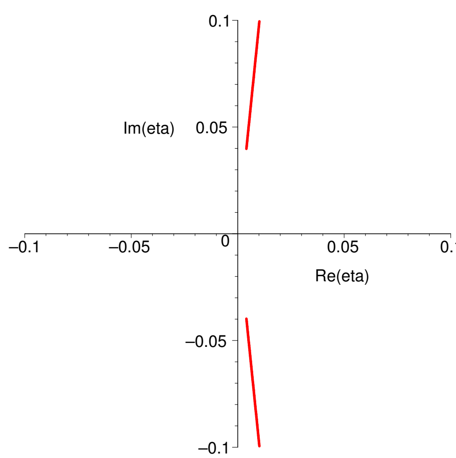

(c) η-plane

Figure 6.4: A different convention for the branch cuts of the theory $\mathcal{A}[g_1, g_2]$. Rotating the cuts permits to analytically continue the definition of the free energy to the left low-temperature ξ half-plane, but it is impossible to reach the real negative axis as happens in Ising.

Amplitude	Integration*	TCS^{1*}	TCS^2	Exact
Γ_{11}^{2+}	0.093(9)	0.093(7)	0.093(8)	
Γ_{11}^{2-}	0.026(2)	0.026(7)	0.023(7)	
B_{12}		1.59(0)	1.594(7)	1.59427...
B_{21}		1.35(6)	1.33(5)	
B_{32}		2.3(8)	2.5(3)	2.45205...
B_{42}		3.(4)	3.(4)	3.70708...

* Values taken from Ref. [40].

Table 6.1: Amplitudes related to the measure of the free energy

with the results coming from integration of the correlation function and TCS applied to the theory Eq. 6.26.

Another interesting possibility offered by the TCS applied on doubly perturbed conformal theories is to follow the renormalization group flow from one theory to another, as illustrated in Fig. 6.5. By turning on a magnetic field φ_1, it is possible to see the four particles under threshold of the theory $\mathcal{A}_2^+$ as they gradually become the three particles of the spectrum of $\mathcal{A}_1$. Around the point $\xi = 0.8$ the mass m_4 disappears as it goes above the threshold. Note that for all the levels the leading mass correction is quadratic in the magnetic field: this is not surprising, since the linear correction to the mass is related to the two-particle form factor [71] of the field φ_1, that vanishes for symmetry reasons. Another effect of the spin-reversal symmetry is evident in the different sign that the leading correction has depending on the mass being even or odd. The ratio between the leading corrections to the masses m_1 and m_2 is a universal quantity

$$\frac{\delta m_2}{\delta m_1} = -0.685(8) \tag{6.28}$$

which would not be easily computed in form factor approach since it involves three-particles form factors. The other two universal ratios

$$\frac{\delta m_3}{\delta m_1} = 6.6(4) \qquad\qquad \frac{\delta m_4}{\delta m_1} = -5.2(6) \tag{6.29}$$

are one order of magnitude less precise.

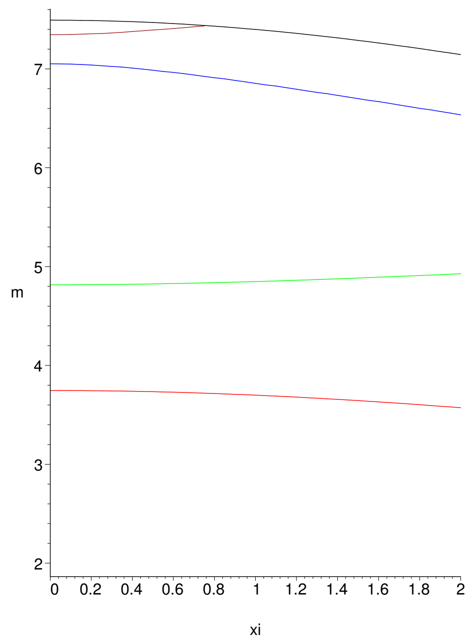

Figure 6.5: Mass spectrum evolution: from $\mathcal{A}_2^+$ to $\mathcal{A}_1$. The black line is the threshold $2m_1$. The four coloured lines represents the stable masses.

Chapter 7

Conclusions

In the spirit of a recent paper by Fonseca and Zamolodchikov [3], I have studied the analytic properties of the free energy of the tricritical Ising model. This minimal model of conformal field theory is characterized by four relevant primary operators, that can be interpreted as a leading and a subleading magnetic fields, a thermal and a chemical potential perturbations.

The main technical tool of my research is the truncation of conformal space, an approximate technique that gives access to the spectrum of the perturbed conformal field theory put on a cylinder. Such a numerical method is the only way we know to get nonperturbative data about nonintegrable field theories. The main limitation of TCS is its bad performance when dealing with perturbations originated by relevant fields whose conformal dimension is near to or greater than $1/2$. This failure is inherent to the approach, so we cannot expect to be able to probe by means of it the behavior of the free energy far from the plane $g_3 = g_4 = 0$.

Such plane can indeed be studied, and the results of my inspection brings some expected facts and some surprising ones. The high-temperature sector exhibits a pair of Lee–Yang-like edge singularities on the imaginary axis of the magnetic field, like the simpler Ising model. The nonunitary minimal model related to the critical process of accumulation of the zeros of the partition function could be $\mathcal{M}(7,2)$, as claimed by von Gehlen [66], but I failed in producing some euristhic theoretical argument in favor of his numerical finite-size-scaling results. The direct computation of the effective central charge associated to the renormalization group flow is within the possibility of TCS, but requires an heavy increase in computational cost that I did not pursue yet.

On the side of the surprising results, there is an interesting difference with respect to the Ising prototype. In the low-temperature regime, due to the different conformal dimensions of the operators involved, it is not possible, starting from the positive real magnetic field axis, to analytically continue the definition of the free energy until reaching the negative real axis. It seems appealing to identify the two unexpected branching points that appear in the left half-plane with a pair of complex conjugate spinoidal singularities. This identification, much in the spirit of the extended analyticity conjecture proposed by Fonseca and Zamolodchikov, opens a problem of physical interpretation I would like to address in the near future.

I tried to enlarge the analysis by including also the coupling g_4. An euristhic argument, based on the physical interpretation of g_4 and on the existence of a massless renormalization group flow from TIM to Ising field theory along the φ_4 perturbation, suggests what may be the extension of my results to the three dimensional space identified by $g_3 = 0$. As far as this conjecture can be numerically tested by TCS – that is not very far, to be honest – it seems to hold. By increasing the level of truncation one can hope to probe also the g_3 direction, but a huge computational effort will be required.

As a byproduct of my work on the analytic properties, I could compute some susceptibilities and vacuum expectation values already evaluated by means of a slightly different use of TCS, thus obtaining an internal consistency check. Moreover, I studied the evolution of the mass spectrum of the theory deformed by the leading energy perturbation (in the high-temperature regime) when a small magnetic field is introduced. The universal ratios between mass corrections have been determined for the first time.

Appendix A

About the energy-momentum tensor

Consider a field theory defined by an action $\mathcal{A}$ on a D-dimensional manifold equipped with metric tensor $g_{\mu\nu}(x)$. If we perform a general infinitesimal transformation of the coordinates $x^\mu \to \tilde{x}^\mu = x^\mu + \varepsilon^\mu$, the corresponding change for the metric tensor is $g_{\mu\nu}(x) \to \tilde{g}_{\mu\nu}(\tilde{x})$, with

$$\tilde{g}_{\mu\nu} = \frac{\partial x^\rho}{\partial \tilde{x}^\mu} \frac{\partial x^\sigma}{\partial \tilde{x}^\nu} g_{\rho\sigma} \,, \tag{A.1}$$

that to first order in ε reads

$$\tilde{g}_{\mu\nu} = g_{\mu\nu} - (\partial_\mu \varepsilon_\nu + \partial_\nu \varepsilon_\mu) \,. \tag{A.2}$$

The classical energy-momentum tensor is defined as the functional derivative of the action with respect to the metric, evaluated in flat space:

$$\delta\mathcal{A} = -\frac{1}{2} \int d^D x \, T^{\mu\nu} \delta g_{\mu\nu} \,. \tag{A.3}$$

The above definition can be generalized to the quantum case in the following way: consider the partition function

$$Z[g] = \int \mathcal{D}_g \Phi \, \exp(-\mathcal{A}[\Phi, g]) = \exp(-\mathcal{W}[g]) \,, \tag{A.4}$$

where Φ stands for the set of dynamical fields of the theory, and $\mathcal{W}$ is the connected functional, that is the field theory equivalent of the free energy f defined by Eq. (1.3). Note that the functional integration measure $\mathcal{D}_g(\Phi)$ depends on the metric. Now the quantum energy-momentum tensor is defined by performing an infinitesimal variation of the metric $g_{\mu\nu} \to \delta g_{\mu\nu}$:

$$Z[g + \delta g] = \int \mathcal{D}_g \Phi \, \exp(-\mathcal{A}[\Phi, g]) \left\{ 1 + \frac{1}{2} \int d^D x \, \sqrt{|g|} \delta g_{\mu\nu} T^{\mu\nu} \right\} \,, \tag{A.5}$$

where the important point is that the energy-momentum tensor takes care of the variation of both the action and the integration measure. Equation (A.5) can be rewritten in the form

$$\delta\mathcal{W}[g] = -\frac{1}{2}\int d^Dx\,\sqrt{|g|}\delta g_{\mu\nu}\langle T^{\mu\nu}\rangle\,, \tag{A.6}$$

where the vacuum expectation value is defined as usual

$$\langle T^{\mu\nu}(\Phi)\rangle = \frac{1}{Z[g]}\int \mathcal{D}_g\Phi\, T^{\mu\nu}(\Phi)\exp(-\mathcal{A}[\Phi,g])\,. \tag{A.7}$$

Appendix B

The edge singularity in Ising and Tricritical Ising

The Yang–Lee edge singularity in the Ising model is described by the conformal theory $\mathcal{M}(5,2)$. As the tricritical Ising model is the next simplest unitary minimal model, its edge singularity is expected to be related with 'the next simplest nonunitary' minimal model. Which theory deserves such title, however, is not univocally clear. Keeping one of the labels unchanged, one could think $\mathcal{M}(5,3)$ or $\mathcal{M}(7,2)$ to be good candidates. As observed by von Gehlen [66], $\mathcal{M}(8,5)$ too is near the $\mathcal{M}(5,2)$ model, at least in the sense of the renormalization group flow caused by the $\phi_{(1,3)}$ perturbation [72]. The main properties of these three candidates are briefly recalled in the next section.

On the base of his finite-size-scaling study [66] of the Blume–Capel model, von Gehlen claims that the correct model should be $\mathcal{M}(7,2)$. It would be quite interesting to be able to confirm (or confute) his identification by independent methods. As I wrote in Sec. 6.3.1, the direct approach to the problem is to locate as precisely as possible the critical value of ξ, then to study the r-dependence of the lowest eigenvalue of the Hamiltonian $\mathcal{H}_+(\xi_c)$: the leading term is proportional to r, the subleading one goes like $1/r$ and its coefficient gives the effective central charge of the field theory associated to the critical point.

This route was followed by Fonseca and Zamolodchikov [3] in studying the edge singularity of the Ising model. In fact, the precision of the truncated fermion space approach they used is so high that they were able to estimate even the coefficient of the sub-subleading term ($\propto 1/r^2$)! When trying to treat in the same way the tricritical Ising, one realizes all the limitations of TCS: at level 5 of truncation (228 states), the position of the critical point itself cannot be determined with more than three digits (against the

0	$-\frac{1}{20}$	$\frac{1}{5}$	$\frac{3}{4}$
$\frac{3}{4}$	$\frac{1}{5}$	$\frac{-1}{20}$	0

Table B.1: Kac table of the minimal model $\mathcal{M}(5,3)$

$\phi_{(1,2)} \times \phi_{(1,2)} = \phi_{(1,1)} + \phi_{(1,3)}$	$\phi_{(1,3)} \times \phi_{(1,3)} = \phi_{(1,1)} + \phi_{(1,3)}$
$\phi_{(1,2)} \times \phi_{(1,3)} = \phi_{(1,2)} + \phi_{(1,4)}$	$\phi_{(1,3)} \times \phi_{(1,4)} = \phi_{(1,2)}$
$\phi_{(1,2)} \times \phi_{(1,4)} = \phi_{(1,3)}$	$\phi_{(1,4)} \times \phi_{(1,4)} = \phi_{(1,1)}$

Table B.2: Fusion rules of the minimal model $\mathcal{M}(5,3)$

five significant digits of Ref. [3]). In principle, however, there is nothing to prevent us from truncating at higher levels until we reach the desired precision.

Instead of pursuing this purely numerical approach, I tried to generalize the argument originally used by Fisher [13] to guess the correct Landau–Ginzburg description of the Lee–Yang edge singularity. The effective field theory can then (hopely) be associated to the correct minimal model by arguments similar to those employed by Cardy [14]. Actually, my attempt failed, as it is explained in the second section of this appendix.

However, it must be noticed that the operator algebras of both the models $\mathcal{M}(5,3)$ and $\mathcal{M}(8,5)$ exhibit symmetries (see App. B) that one would not expect to find, since the field φ_1 breaks all the symmetries present at the conformal point.

B.1 Non-unitary minimal models

B.1.1 $\mathcal{M}(5,3)$

This model has central charge $c = -3/5$ and effective central charge $\tilde{c} = 3/5$. Its Kac table is reported in Tab. B.1, and the fusion rules in Tab. B.2. Note that the fusion rules are compatible with a $\mathbb{Z}_2$ symmetry: $\phi_{(1,1)}$ and $\phi_{(1,3)}$ are even, while $\phi_{(1,2)}$ and $\phi_{(1,4)}$ are odd.

0	$-\frac{2}{7}$	$-\frac{3}{7}$	$-\frac{3}{7}$	$-\frac{2}{7}$	0

Table B.3: Kac table of the minimal model $\mathcal{M}(7,2)$

$\phi_{(1,2)} \times \phi_{(1,2)} = \phi_{(1,1)} + \phi_{(1,3)}$	$\phi_{(1,3)} \times \phi_{(1,3)} = \phi_{(1,1)} + \phi_{(1,2)}$
$\phi_{(1,2)} \times \phi_{(1,3)} = \phi_{(1,2)} + \phi_{(1,3)}$	

Table B.4: Fusion rules of the minimal model $\mathcal{M}(7,2)$

B.1.2 $\mathcal{M}(7,2)$

The minimal model $\mathcal{M}(7,2)$ is characterized by central charge $c = -68/7$ and effective central charge $\tilde{c} = 4/7$. This model has attracted some attention [71] because of its very simple dynamics: there are only two relevant fields, and the corresponding perturbations are both integrable. The Kac table is given in Tab. B.3, and Tab. B.4 shows the fusion rules. It is easy to realize that the operator algebra of this model doesn't allow any symmetry among the fields. This lack of symmetry is just what we expect when using the field σ to go off the critical point in the tricritical Ising model. This argument is not a proof, but if considered together with the numerical results of Ref. [66], somewhat supports the hypothesis that $\mathcal{M}(7,2)$ is indeed the right 'next simplest nonunitary' minimal model associated with the edge singularity of TIM.

B.1.3 $\mathcal{M}(8,5)$

The minimal model $\mathcal{M}(8,5)$, characterized by central charge $c = -7/20$ and effective central charge $\tilde{c} = 17/20$, is less intuitively 'simple', because of its large Kac table (Tab B.5) and rich operator algebra, which I omit. Also this model possesses an internal symmetry, as is signaled by the fact that $\phi_{(1,1)}, \phi_{(1,3)}, \phi_{(1,5)}, \phi_{(1,7)}$ form a subalgebra.

B.2 Effective field theory

Let us first recall how the edge singularity of the Ising model was identified with the minimal model $\mathcal{M}(5,2)$. The argument used by Fisher [13] can be

0	$-\frac{1}{32}$	$\frac{1}{4}$	$\frac{27}{32}$	$\frac{7}{4}$	$\frac{95}{32}$	$\frac{9}{2}$
$\frac{7}{10}$	$\frac{27}{160}$	$-\frac{1}{20}$	$\frac{7}{160}$	$\frac{9}{20}$	$\frac{187}{160}$	$\frac{11}{5}$
$\frac{11}{5}$	$\frac{187}{160}$	$\frac{9}{20}$	$\frac{7}{160}$	$-\frac{1}{20}$	$\frac{27}{160}$	$\frac{7}{10}$
$\frac{9}{2}$	$\frac{95}{32}$	$\frac{7}{4}$	$\frac{27}{32}$	$\frac{1}{4}$	$-\frac{1}{32}$	0

Table B.5: Kac table of the minimal model $\mathcal{M}(8,5)$

summarized as follows: Let Φ be the order parameter for a system whose free energy admits an effective description in terms of the Landau–Ginzburg potential

$$V(\Phi) = g_1\Phi + g_2\Phi^2 + \Phi^4 \,. \tag{B.1}$$

The coupling are interpreted as a magnetic field (g_1) and a reduced temperature (g_2). A critical point is characterized by the condition $g_1 = g_2 = 0$. If we now shift the field by an imaginary constant:

$$\Phi(x) \to \widetilde{\Phi}(x) + i\Phi_0 \,, \tag{B.2}$$

then the effective potential becomes

$$V'(\widetilde{\Phi}) = \widetilde{\Phi}_0 + [g_1 - 2i\Phi_0(\Phi_0^2 - g_2)]\widetilde{\Phi} + [g_2 - 6\Phi_0^2]\widetilde{\Phi}^2 + 4i\Phi_0\widetilde{\Phi}^3 + \widetilde{\Phi}^4 \,, \tag{B.3}$$

where $\widetilde{\Phi}_0$ is an unimportant constant factor. We can fix Φ_0 in such a way that the critical behavior is preserved, that is by requiring that the coefficient of $\widetilde{\phi}^2$ vanishes. After the substitution $\Phi_0 = \pm\sqrt{g_2/6}$, we are left with

$$V'(\widetilde{\Phi}) = \widetilde{\Phi}_0 + [g_1 \pm i(2g_2/3)^{3/2}]\widetilde{\Phi} \pm 2i(2g_2/3)^{3/2}\widetilde{\Phi}^3 + \widetilde{\Phi}^4 \,. \tag{B.4}$$

From this expression Fisher guessed the correct effective theory for the Yang–Lee singularity:

$$\mathcal{L}_{\mathrm{YL}} = \frac{1}{2}(\partial_\mu\Phi)^2 + i(g_1 - h_c)\Phi + i\gamma\Phi^3 \,, \tag{B.5}$$

with h_c and γ real.

The last equation is the starting point for the following argument, due to Cardy [14], which identifies the correct minimal model related to this critical phenomenon. The classical equation of motion of the Lagrangian (B.5) is

$$\partial_\mu^2\Phi = i3\gamma\Phi^2 + i(h - h_c) \,. \tag{B.6}$$

This implies that the composite field Φ^2 is indeed redundant in renormalization group sense: it is just a derivative of Φ and doesn't give rise to any new scaling field. In the language of fusion rules, this is written

$$\Phi \times \Phi = \mathbb{I} + \Phi \,. \tag{B.7}$$

The only non-unitary minimal model which has just one operator besides the identity is $\mathcal{M}(5,2)$.

The simplest way to generalize Fisher's argument is probably too naïve: let's try to replace the effective potential (B.1) with the Φ^6 potential already introduced in Sec. 1.2:

$$V(\Phi) = g_1\Phi + g_2\Phi^2 + g_3\Phi^3 + g_4\Phi^4 + \Phi^6 \,. \tag{B.8}$$

The tricritical point is characterized by the condition $g_1 = g_2 = g_3 = g_4 = 0$. Under the shift (B.2) of the order parameter, the effective potential (B.8) is rewritten

$$\begin{aligned} V'(\widetilde{\Phi}) = \widetilde{\Phi}_0 &+ [g_1 - 3g_3\Phi_0^2 + 2i\Phi_0(g_2 - 2g_4\Phi_0^2 + 3\Phi_0^4)]\widetilde{\Phi} \\ &+ [g_2 - 6g_4\Phi_0^2 + 15\Phi_0^4 + 3ig_3\Phi_0]\widetilde{\Phi}^2 + [g_3 + 4ig_4\Phi_0 - 20i\Phi_0^3]\widetilde{\Phi}^3 \\ &+ [g_4 - 15\phi_0^2]\widetilde{\Phi}^4 + 6i\Phi_0\widetilde{\Phi}^5 + \widetilde{\Phi}^6 \,, \end{aligned} \tag{B.9}$$

where $\widetilde{\Phi}_0$ is a constant. In order to recover a tricritical behavior, we may choose Φ_0 in such a way that the coefficient of $\widetilde{\Phi}^4$ vanishes, then dispose of g_2 in order to eliminate the coefficient of $\widetilde{\Phi}^2$: one would end up with the effective Lagrangian for the Lee–Yang-like edge singularity

$$\mathcal{L}_{\mathrm{LYl}} = \frac{1}{2}(\partial_\mu\Phi)^2 + (g_1 - ih_c)\Phi + (g_3 - ih'_c)\Phi^3 + i\gamma\Phi^5 \,, \tag{B.10}$$

where both h_c, h'_c are functions of the coupling γ.

This procedure is quite arbitrary. Why not fixing also g_3, thus obtaining

$$\mathcal{L}'_{\mathrm{LYl}} = \frac{1}{2}(\partial_\mu\Phi)^2 + (g_1 - ih_c)\Phi + i\gamma\Phi^5 \,. \tag{B.11}$$

In point of fact, these kind of arguments are far by rigorous, and can be useful only when they inspire a guess that can be verified by other means. In this case, there seems to be no intuitive way of relating neither Eq. (B.10) nor Eq. (B.11) to one of the fusion rules sets represented in Tabs. B.4 and B.2.

Acknowledgements

I would like to thank Aldo Delfino, Giovanni Feverati, and Paolo Grinza for having shared their insight in many valuable discussions. I had the luck to find here in SISSA an unusually large group of people researching about the same topics: I greatly appreciated the possibility of working with them.

In questi quattro anni molte persone mi hanno sopportato con ammirevole pazienza, degna forse di miglior causa: mi pare doveroso ringraziarle. Quelli che mi hanno sopportato di piú sono stati i miei cari amici Herr Doktor Cinghiale e Mahatma Javarnanda (ELO rating 1555): insieme abbiamo gestito la Stanza 30 con grande efficienza, mantenendo sempre un certo livello, anche se medio-basso. Non so quando ci capiterà di nuovo di ritrovarci insieme tutti e tre, ma quando capiterà sarà un bel giorno.

Naturalmente, la Stanza 30 non sarebbe mai potuta diventare quello splendido ambiente cosí commoventemente inadatto al lavoro che è stata senza la collaborazione degli altri suoi frequentatori abituali: Fabbio (ELO rating 1450), l'inarrivabile Decano degli Studenti, il Cignale della Val Brembana, per citare solo i piú incalliti. Un grazie di cuore anche a loro.

Un saluto affettuoso al Bestiame, che ha molto alleviato la deprimente Triestezza delle serate spese in questa città che non mi è affatto congeniale: in primis al *maestro de vida* Dottor Bolzicco e al Sub-Comandante Ingegner Nicola, per tacer del Vacca, Vito, Simone, l'Interlocutrice Comunista, il Moskiz, Piero, il Coccolo, Paolo. E un grazie particolare alla Sfattona. Tutti personaggi, ci tengo a sottolineare, di grandissimo rilievo.

Grazie a Gentalyn, Zerinol, Psycopsy (o Fluwoeb che dir si voglia) che mi hanno sopportato come Master. Grazie ad Angelo, Husam, Dario ed Elisa che mi hanno sopportato come coinquilino. Grazie al Cascella (non stiamo mica parlando del Mutandari) che mi ha sopportato durante i concerti. Grazie a tutti i sissaioli che se mi metto a nominarli uno per uno raggiungo finalmente le cento pagine che avrebbe voluto il mio relatore.

Poi un grazie agli amici lontani, che mi sopportano solo pochi giorni l'anno ma mi sopporterebbero volentieri anche di piú: il Vax, Chris, Musacchio, il Fanfa, la Bbona, Davide, Fede e il Barta, Toni, Lops e i romani che, mannaggia, ci si potesse vedere piú spesso, chissà cosa potremmo combinare. Grazie a Cristian e a tutta la compagnia di D.I.R.A.C., perché è stata una grande esperienza per me, anche se sono arrivato solo all'ultimo momento.

Grazie alle mie migliori amiche: Lola, Ligeia e Vic. Dovunque mi porti questo lavoro, non ci perderemo mai di vista, ve l'ho promesso nove anni fa a Santa Maria degli Angeli e sono uno che mantiene le promesse.

Grazie a Fokker perché mi ha fatto incontrare Artemis, e ad Artemis per avermi tolto la maschera e non essersi spaventata di quello che c'era dietro.

Bibliography

[1] C. N. Yang and T. D. Lee. Statistical theory of equations of state and phase transitions. I. Theory of condensation. *Phys. Rev.*, 87(3):404–409, August 1952.

[2] T. D. Lee and C. N. Yang. Statistical theory of equations of state and phase transitions. II. Lattice gas and Ising model. *Phys. Rev.*, 87(3):410–419, August 1952.

[3] P. D. Fonseca and A. Zamolodchikov. Ising field theory in a magnetic field: Analytic properties of the free energy. *J. Stat. Phys.*, 110(3-6):527–590, March 2003.

[4] H. A. Kramers and G. H. Wannier. Statistics of the two-dimensional ferromagnet. Part I. *Phys. Rev.*, 60(3):252–262, August 1941.

[5] H. A. Kramers and G. H. Wannier. Statistics of the two-dimensional ferromagnet. Part II. *Phys. Rev.*, 60(3):263–276, August 1941.

[6] M. Blume, V. J. Emery, and R. B. Griffiths. Ising model for the lambda transition and phase separation in He^3-He^4 mixtures. *Phys. Rev. A*, 4(3):1071–1077, September 1971.

[7] M. Blume. Theory of the first-order magnetic phase change in UO_2. *Phys. Rev.*, 141(2):517–524, January 1966.

[8] H. W. Capel. On the possibility of first-order phase transitions in Ising systems of triplet ions with zero-field splitting. *Physica*, 32:966–988, 1966.

[9] I. D. Lawrie and S. Sarbach. Theory of tricritical points. In C. Domb and J. L. Lebowitz, editors, *Phase Transitions and Critical Phenomena*, volume 9, chapter 1, pages 1–161. Academic Press, London, 1984.

[10] D. Furman, S. Dattagupta, and R. B. Griffiths. Global phase diagram for a three-component model. *Phys. Rev. B*, 15(1):441–464, January 1977.

[11] L. D. Landau, E. M. Lifshits, and L. P. Pitaevskii. *Statistical Physics Part I*, chapter XIV. Number 5 in Course of Theoretical Physics. Pergamon Press, 3rd edition, 1980.

[12] R. B. Griffiths. Thermodynamic model for tricritical points in ternary and quaternary fluid mixtures. *J. Chem. Phys.*, 60(1):195–206, January 1974.

[13] M. E. Fisher. Yang-Lee edge singularity and ϕ^3 field theory. *Phys. Rev. Lett.*, 40(25):1610–1613, June 1978.

[14] J. L. Cardy. Conformal invariance and the Yang–Lee edge singularity in two dimensions. *Phys. Rev. Lett.*, 54(13):1354–1356, April 1985.

[15] J. S. Langer. Theory of the condensation point. *Ann. Phys.*, 41(1):108–157, January 1967. Reprinted in *Ann. Phys.*, 281:941–990, 2000.

[16] W. P. Orrick, B. Nickel, A. J. Guttmann, and J. H. H. Perk. The susceptibility of the square lattice Ising model: New developments. *J. Stat. Phys.*, 102(3/4):795–841, February 2001.

[17] P. Di Francesco, P. Mathieu, and D. Sénéchal. *Conformal Field Theory*. Springer, 1996.

[18] P. Ginsparg. Applied conformal field theory. In E. Brézin and J. Zinn-Justin, editors, *Fields, Strings and Critical Phenomena*, pages 1–168. Elsevier, 1989.

[19] C. Itzykson and J.-M. Drouffe. *Statistical Field Theory*. Cambridge University Press, 1989.

[20] G. Mussardo. Off-critical statistical models: Factorized scattering theories and bootstrap program. *Phys. Rep.*, 218(5,6):215–379, 1992.

[21] A. A. Belavin, A. M. Polyakov, and A. B. Zamolodchikov. Infinite conformal symmetry in two-dimensional quantum field theory. *Nucl. Phys. B*, 241(2):333–380, July 1984.

[22] A. Rocha-Caridi. Vacuum vector representations of the virasoro algebra. In James Lepowsky, Stanley Mandelstam, and I. M. Singer, editors, *Vertex Operators in Mathematics and Physics*, number 3 in Mathematical

Sciences Research Institute Publications, pages 451–473. Mathematical Sciences Research Institute, Springer-Verlag, 1985.

[23] J. Cardy. Operator content of two-dimensional conformally invariant theories. *Nucl. Phys. B*, 270(2):186–204, June 1986.

[24] A. Cappelli, C. Itzykson, and J.-B. Zuber. Modular invariant partition functions in two dimensions. *Nucl. Phys. B*, 280(3):445–465, March 1987.

[25] A. Cappelli, C. Itzykson, and J.-B. Zuber. The A-D-E classification of minimal and $a_1^{(1)}$ conformal invariant theories. *Commun. Math. Phys.*, 113(1):1–26, 1987.

[26] A. Kato. Classification of modular invariant partition functions in two dimensions. *Mod. Phys. Lett. A*, 2(8):585–600, August 1987.

[27] A. B. Zamolodchikov. Integrals of motion in scaling 3-state Potts model field theory. *Int. J. Mod. Phys. A*, 3(3):743–750, March 1988.

[28] A. B. Zamolodchikov. Integrable field theory from conformal field theory. In M. Jimbo, T. Miwa, and A. Tsuchiya, editors, *Integrable Systems in Quantum Field Theory and Statistical Mechanics*, number 19 in Advanced Studies in Pure Mathematics, pages 641–674. Academic Press, November 1989.

[29] S. Parke. Absence of particle production and factorization of the s-matrix in $1+1$ dimensional models. *Nucl. Phys. B*, 174(1):166–182, November 1980.

[30] H. Babujian and M. Karowski. The "bootstrap program" for integrable quqantum field theories in $1+1$ dimensions. In V. G. Gurzadyan and A. G. Sedrakian, editors, *From Integrable Models to Gauge Theories: A Volume in Honor of Sergei Matinyan*, pages 53–76. World Scientific, 2002.

[31] F. A. Smirnov. *Form Factors in Completely Integrable Models of Quantum Field Theory.* Number 14 in Advanced Series in Mathematical Physics. World Scientific, 1992.

[32] G. Delfino and G. Mussardo. The spin-spin correlation function in the two-dimensional Ising model in a magnetic field at $t = t_c$. *Nucl. Phys. B*, 455(3):724–758, November 1995.

[33] Al. B. Zamolodchikov. Two-point correlation function in scaling Lee–Yang model. *Nucl. Phys. B*, 348(3):619–641, January 1991.

[34] M. Lässig, G. Mussardo, and J. L. Cardy. The scaling region of the tricritical Ising model in two dimensions. *Nucl. Phys. B*, 348(3):591–618, January 1991.

[35] A. B. Zamolodchikov. Conformal symmetry and multicritical points in two-dimensional quantum field theory. *Sov. J. Nucl. Phys.*, 44(3):529–533, September 1986.

[36] Vl. S. Dotsenko and V. A. Fateev. Conformal algebra and multipoint correlation functions in 2d statistical models. *Nucl. Phys. B*, 240(3):312–348, October 1984.

[37] Vl. S. Dotsenko and V. A. Fateev. Four-point correlation functions and the operator algebra in 2d conformal invariant theories with central charge $c \leq 1$. *Nucl. Phys. B*, 251(5/6):691–734, May 1985.

[38] C. Acerbi, A. Valleriani, and G. Mussardo. Form factors and correlation functions of the stress-energy tensor in massive deformation of the minimal models $(e_n)_1 \otimes (e_n)_1/(e_n)_2$. *Int. J. Mod. Phys. A*, 11(30):5327–5364, December 1996.

[39] D. Friedan, Z. Qiu, and S. Shenker. Superconformal invariance in two dimensions and the tricritical Ising model. *Phys.Lett.B*, 151(1):37–43, January 1985.

[40] D. Fioravanti, G. Mussardo, and P. Simon. Universal amplitude ratios of the renormalization group: Two-dimensional tricritical Ising model. *Phys. Rev. E*, 63:016103, December 2000.

[41] P. Christe and G. Mussardo. Integrable systems away from criticality: The Toda field theory ans s-matrix of the tricritical Ising model. *Nucl. Phys. B*, 330(2/3):465–487, January 1990.

[42] V. A. Fateev and A. B. Zamolodchikov. Conformal field theory and purely elastic s-matrices. *Int. J. Mod. Phys. A*, 5(6):1025–1048, March 1990.

[43] V. A. Fateev. The exact relations between the coupling constants and the masses of particles for the integrable perturbed conformal fiedld theories. *Phys.Lett.B*, 324(1):45–51, March 1994.

[44] F. A. Smirnov. Exact s-matrices for $\phi_{1,2}$-perturbated minimal models of conformal field theory. *Int. J. Mod. Phys. A*, 6(8):1407–1428, March 1991.

[45] F. Colomo, A. Koubek, and G. Mussardo. On the s-matrix of the subleading magnetic deformation of the tricritical Ising model in two dimensions. *Int. J. Mod. Phys. A*, 7(21):5281–5305, August 1992.

[46] A. B. Zamolodchikov. Thermodynamic bethe ansatz for rsos scattering theories. *Nucl. Phys. B*, 358(3):497–523, July 1991.

[47] D. A. Kastor, E. J. Martinec, and S. H. Shenker. RG flow in $n = 1$ discrete series. *Nucl. Phys. B*, 316(3):590–608, April 1989.

[48] Al. B. Zamolodchikov. From tricritical ising to critical ising by thermodynamic bethe ansatz. *Nucl. Phys. B*, 358(3):524–546, July 1991.

[49] G. Delfino, G. Mussardo, and P. Simonetti. Correlation functions along a massless flow. *Phys. Rev. D*, 51(12):6620–6624, June 1995.

[50] G. Delfino. First-order phase transition and integrable field theory. the dilute q-state Potts model. *Nucl. Phys. B*, 554:537–551, 1999.

[51] Al. B. Zamolodchikov. Thermodynamic bethe ansatz in relativistic models: Scaling 3-state Potts and Lee–Yang models. *Nucl. Phys. B*, 342(3):695–720, October 1990.

[52] C. N. Yang. Some exact results for the many-body problem in one dimension with repulsive delta-function interaction. *Phys. Rev. Lett.*, 19(23):1312–1315, December 1967.

[53] V. P. Yurov and Al. B. Zamolodchikov. Truncated conformal space approach to scaling Lee–Yang model. *Int. J. Mod. Phys. A*, 5(16):3221–3245, August 1990.

[54] H. W. J. Blöte, J. L. Cardy, and M. P. Nightingale. Conformal invariance, the central charge, and universal finite-size amplitudes at criticality. *Phys. Rev. Lett.*, 56(7):742–745, February 1986.

[55] I. Affleck. Universal term in the free energy at a critical point and the conformal anomaly. *Phys. Rev. Lett.*, 56(7):746–748, February 1986.

[56] M. Lässig and G. Mussardo. Hilbert space and structure constants of descendant fields in two-dimensional conformal field theories. *Comp. Phys. Comm.*, 66:71–88, 1991.

[57] M. E. Fisher. volume VIIC of *Lectures in Theoretical Physics*, pages 1–. University of Colorado Press, Boulder.

[58] G. L. Jones. Complex temperatures and phase transitions. *J. Math. Phys.*, 7(11):2000–2005, November 1966.

[59] J. Balog, M. Niedermaier, F. Niedermayer, A. Patrascioiu, E. Seiler, and P. Weisz. The intrinsic coupling in integrable quantum field theories. *Nucl. Phys. B*, 583:614–670, 2000.

[60] V. Fateev, S. Lukyanov, A. B. Zamolodchikov, and Al. B. Zamolodchikov. Expectation values of local fields in the Bullough–Dodd model and integrable perturbed conformal field theories. *Nucl. Phys. B*, 516:652–674, 1998.

[61] M. Suzuki. Theorems on extended Ising model with applications to dilute ferromagnetism. *Progr. Theor. Phys.*, 40(6):1246–1256, December 1968.

[62] S. Sarbach and F. Rys. Domain of zeros of the partition function for some magnetic lattice systems. *Phys. Rev. B*, 7(7):3141–3143, April 1973.

[63] K. Y. Millard and K. S. Viswanathan. Upper bounds on critical temperature and magnetic field for a class of Ising spin-1 models. *Phys. Rev. B*, 9(5):2030–2035, March 1974.

[64] M. Biskup, C. Borgs, J. T. Chayes, L. J. Kleinwaks, and R. Kotecký. General theory of Lee-Yang zeros in models with first-order phase transitions. *Phys. Rev. Lett.*, 84(21):4794–4797, May 2000.

[65] M. Biskup, C. Borgs, J. T. Chayes, and R. Kotecký. Partition function zeros at first order phase-transitions: Pirogov–Sinai theory. *J. Stat. Phys.*, 116(1–4):97–155, August 2004.

[66] G. von Gehlen. Non-Hermitian tricriticality in the Blume–Capel model with imaginary field. *Int. J. Mod. Phys. B*, 8(25,26):3507–3529, 1994.

[67] Y. Gefen, Y. Imry, and D. Mukamel. Phase diagram of spin-1 quantum Ising models: Application to systems of weakly coupled classical Ising chains. *Phys. Rev. B*, 23(11):6099–6105, June 1981.

[68] N. J. Günther, D. A. Nicole, and D. J. Wallace. Goldstone modes in vacuum decay and first-order phase transitions. *J. Phys. A*, 13:1755–1767, 1980.

[69] M. San Miguel and J. D. Gunton. Metastability in tricritical system. *Phys. Rev. B*, 23(5):2317–2333, March 1981.

[70] R. Guida and N. Magnoli. Vacuum expectation values from a variational approach. *Phys. Lett. B*, 411:127–133, October 1997.

[71] G. Delfino, G. Mussardo, and P. Simonetti. Non-integrable quantum field theories as perturbations of certain integrable models. *Nucl. Phys. B*, 473:469–508, 1996.

[72] M. Lässig. New hierarchies of multicriticality in two-dimensional field theory. *Phys.Lett.B*, 278(4):439–442, April 1992.